DESIGN OF TRUSS-LIKE CELLULAR STRUCTURES USING

DENSITY INFORMATION FROM TOPOLOGY OPTIMIZATION

A Thesis
Presented to
The Academic Faculty

By

Mahmoud Alzahrani

In Partial Fulfillment
Of the Requirements for the Degree
Master of Science in Mechanical Engineering in the
George W. Woodruff School of Mechanical Engineering

Georgia Institute of Technology
August 2014

DESIGN OF TRUSS-LIKE CELLULAR STRUCTURES USING

DENSITY INFORMATION FROM TOPOLOGY OPTIMIZATION

Approved by:

Dr. Seung-Kyum Choi, Advisor
George W. Woodruff School of Mechanical Engineering
Georgia Institute of Technology

Prof. David W. Rosen
George W. Woodruff School of Mechanical Engineering
Georgia Institute of Technology

Dr. Yan Wang
George W. Woodruff School of Mechanical Engineering
Georgia Institute of Technology

Date Approved: 5/16/2014

I dedicate this thesis to my family for their support and love.

ACKNOWLEDGEMENTS

Tables of Contents

LIST OF TABLES

LIST OF FIGURES

LIST OF ABBREVIATIONS

AM ·· Additive Manufacturing

CAD ·· Computer-Aided Design

DLP ·· Digital Light Processing

FDM ·· Fusion Deposition Modeling

FEM ·· Finite Element Method

GGSM ··· Growing Ground Structure Method

RDM ·· Relative Density Mapping

SLA ·· Stereolithography

SLS ·· Selective Laser Sintering

SUMMARY

The advances in additive manufacturing removed most of the limitations that were once stopping designers when it comes to manufacturing their designs. It allowed designers to produce parts with high geometric complexity, such as cellular structures. These structures are known for their high strength relative to their low mass, good energy absorption, and high thermal and acoustic insulation compared to their relative solid counter-parts. Lattice structures, a type of cellular structures, have received considerable attention due to their properties when producing light-weight with high strength parts. The design of these structures can pose a challenge to designers due to the sheer number of variables that are present. Traditional optimization approaches become an infeasible approach for designing them, which motivated researchers to search for other alternative approaches.

In a research done for optimizing lattice structures, a Size, Matching, and Scaling (SMS) method was developed. The method utilized solid-body finite element analysis results and mapped it on a predefined lattice configuration. The method then underwent various improvements to enhance its performance. The improvements allowed the utilization of various lattice structure configurations and the ability to work on complex shaped geometry. But the dependence on the results of solid-body analysis limited its application to the loading condition it was designed for, while most designers aim to create robust designs that can handle different loads.

In this research, a new method called the Relative Density Mapping (RDM) is presented. The method aims to overcome the limitations of SMS method in the design of lattice structures that are subject to multiple loading conditions. This is done by utilizing

the relative density information form topology optimization of structures that are subjected to the same loading conditions. This allowed the method to overcome the limitation of being dependent on information that is load specific. The mapping of the relative densities to the lattice structure is presented in this research along with examples of the performance of the structure with other design approaches. Results from the examples have shown that the method is able to produce structures that have comparable performance to SMS and also better performance for multiple loading conditions.

CHAPTER 1

INTRODUCTION, BACKGROUND AND MOTIVATION

1.1 Introduction

Recent advancement in additive manufacturing (AM) has allowed designers to achieve designs that are complex in geometry. Cellular structures have benefited from the advances of AM. These type of structures are useful for achieving light-weight but strong structural systems, since they can be designed to contain materials for specific applications where needed. The focus of this research is the design of a particular type of cellular structures known as lattice structures. These structures have shown great capability and are engineered for applications in industry where both light-weight and stiffness are required. The complexity of designing these structures arises with the increase in the number of elements in them. They could contain hundreds or thousands of elements, which would increase the number of design variables to consider. This could pose a problem in the design process, since the sheer number of design variables could pose to be computationally expensive to determine. This can limit the applicability of utilizing these structures for application. This research will present a new method for designing lattice structures by utilizing the relative density information obtained from topology optimization processes. The benefit of the method is that it can reduce the time for designing lattice structures drastically and it can produce structures that can sustain multiple loading conditions.

1.1.1 Background

1.1.1.1 Additive Manufacturing

Additive Manufacturing, also known as direct manufacturing, is a collection of processes that fabricate complicated 3-D objects from 2-D cross-sectional layer data [1]. The process may take a few hours up to a few days to produce the required part depending on its size and precision rate. This enabled parts produced by AM processes to have high geometric, material, and hierarchical complexity [2]. Some of the benefits of are that it has a predictable time for the fabrication of the model even when there are modifications in the design, the number of processes and resources required is significantly less than conventional manufacturing, and it can be used to simplify multi-stage processes [3].

The process begins by using a Computer Aided Design (CAD) system to build the 3-D model of the part. Then the file is converted into a Standard Tessellation Language (STL) file format which represents the surface of the model as an assembly of triangles. The STL file then used to construct the 2-D cross-sectional layer data that will guide the AM process in constructing the part. Figure 1-1 shows the graphical representation of the process.
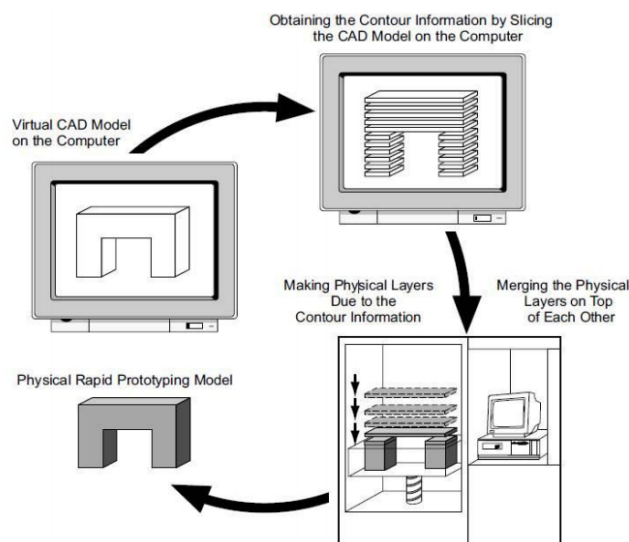
Figure 1-1: Basic model generation by AM process [4]

Some of the commonly used technologies in AM are Stereolithography (SLA), Fused Deposition Modeling (FDM), Selective Laser Sintering (SLS), Digital Light Processing (DLP), and 3-D printing [1].

1.1.1.1.1 Stereolithography (SLA)

SLA is one of the most widely used processes. In SLA, a platform that contains a photocurable polymer, an epoxy or acrylate resin, is contained in a vat of liquid. The data of the 2-D cross-sectional layer is used to guide a low-powered ultraviolet (UV) laser that is used to trace out the cross-section area of the layer curing it within the boundaries until the entire area is solidified. After the first layer, an elevator lowers the platform and a sweeper recoats the solidified layer with liquid polymer. The process then repeats again till the part is complete. Support structures can be used where necessary.

1.1.1.1.2 Fusion Deposition Modeling (FDM)

FDM builds parts from acrylonitrile butadiene styrene (ABS) and other resins that are noted for their toughness which makes it suitable for parts that require durability. It's the second most used process. The process starts with plastic filament being supplied to a heated nozzle that is mounted over a mechanical stage. The nozzle can move horizontally and/or vertically. The nozzle deposits the extruded plastic bead and the support material where needed according to the data from the 2-D layer. The entire process is done in a chamber maintained at a temperature below the melting point of the plastic.

The limitations of FDM arise in the accuracy, material property of the built part and building speed. Since the nozzles are circular in shape, this will affect the final product edges. External and internal corners will have a radius equivalent to that of the nozzle. The produced part will have an anisotropic nature in its property due to the voids that are created in the extrusion process. A controlled layering strategy would reduce this in planes created from the 2-D layers, but not in the direction normal to that plane. The

speed of the process depends on the feed rate which depends on the material being supplied which and the rate at which the liquefier can melt the material to be fed through the nozzle.

1.1.1.1.3 Selective Laser Sintering (SLS)

Similar to SLA, SLS uses the heat of a CO2 laser to create the parts. The material is in powdered form rather than liquid form in a pedestal, which allows the user to choose from a wide range of engineering-grade materials. The laser then turns on and off while scanning through the material (to heat the grains to melt or fusion temperature) selectively sintering the powder. The pedestal is then lowered and a roller then distributes powder over the pedestal surface and the process is repeated until the part is finished. This eliminates the necessity for support structures in SLS. The accuracy and surface finish of the product in SLS is inferior to SLA, and depends on the powder particle size and operating conditions.

1.1.1.1.4 Digital Light Processing (DLP)

DLP, like SLS, uses a photocurable polymer in liquid form contained in a vat. The liquid is subjected to a light source that projects the image of the layer in the liquid to cure the polymer. This eliminates the incremental process of having to scan across the layer to cure the resin, since an entire cross-section is cured at one time. This gives DLP an advantage of speed over the scanning process.

1.1.1.1.5 3-D Printing

3D-printing is considered the most recent process in the market (2007). It can be used to build a part that contains one or two materials simultaneously. It uses Objet Geometries PolyJet Matrix technology. It uses a PolyJet Matrix block, that jets one or two materials in liquid form and gel-like support material, which can be removed by water jetting or by

hand, where needed using fine nozzles and instantly cure them with a UV light mounted on the block. The nozzle design must take into consideration the deposition of the jetted droplets, such as droplet size, velocity, and impact, which may affect the quality of the product. Higher resolution in the part is obtained with small nozzle sizes but they often get clogged which can prevent the droplets from exiting. Monitoring these nozzles is a crucial part in the process.

1.1.1.2 Cellular Solids

Cellular solids are structures with interconnected struts or plates. The struts and plates form the edges and the faces of the cellular solid. These structures contain material where it is needed for specific loading conditions. They are structured as repeated cells, which enables a high degree of optimization that gives designers the ability to control material distribution. The key advantage of cellular structure is their high strength relative to their low mass, good energy absorption, high thermal and acoustic insulation compared to their relative solid counter-parts [5]. They can be a 2-D array of polygons, such as honeycombs, 3-D closed cell foams or 3-D open cell lattice structures. Closed cell foams have the solid faces that separate the cell from neighboring cells, while open cell lattice structures have the cells contained in cell edges so that the cells connect through open faces.
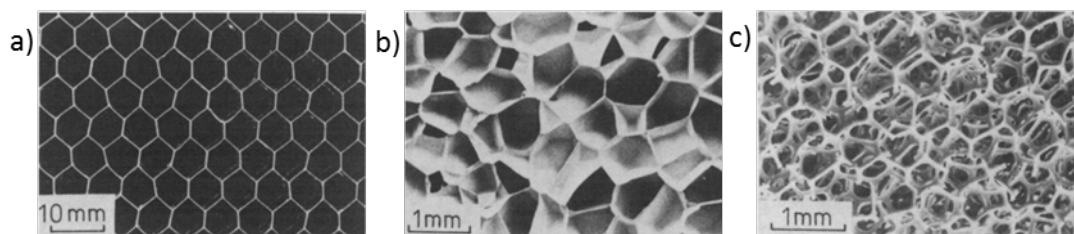
Figure 1-2: Types of cellular solids a) 2-D honeycombs b) 3-D closed cell foams c) 3-D open cell lattice structures [6]

Lattice structures have received considerable attention over foams due to their ability to provide light-weight and stronger materials when compared to foams [7]. Cellular solid strength is governed by its volumetric density ρ_v.

$$\rho_v = \rho^* / \rho_s \qquad (1\text{-}1)$$

where ρ^* is the density of the cellular structure and ρ_s is the density of the solid counter-part of the cellular structure. Studies have shown that the strength of foams is governed by the bending of the face wall that separate the cells in all loading conditions and scales as $\rho_v^{1.5}$. Lattice structures, on the other hand, deform through cell stretching and the strength scales as ρ_v. Thus, for structure with $\rho_v = 0.1$, lattice structures are expected to be three times stronger than foams [8].

<u>1.1.1.3   Structural Optimization</u>

Optimization processes aim to find the best design alternative that will achieve maximum performance for a given objective. With the advances in Finite Element Analysis (FEA), structural optimization approaches are available in commercial FEA packages for users. Structural optimization can be one of five types[9, 10], which are:

1- Shape Optimization
2- Size optimization
3- Topology optimization
4- Topography optimization
5- Topometry optimization

Figure 1-3 shows some of these types of optimization. The following sections will explain these types briefly.

6
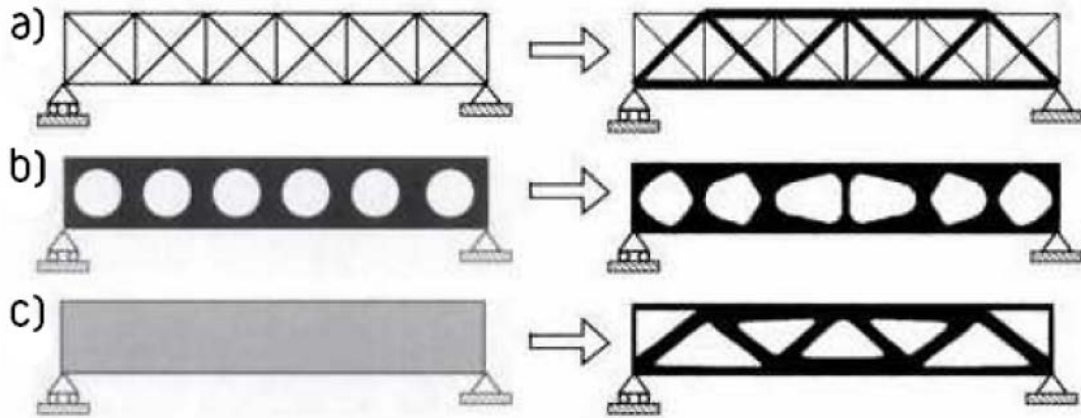
Figure 1-3: Three types of structural optimization a) Size optimization b) Shape optimization

c) Topology optimization [9]

1.1.1.3.1 Shape Optimization

Shape optimization deals with varying specified design variables in the structures, such as fillets, chamfers, radii, etc. The process varies these variables until the design response and constraints are met. Shape optimization does not change the connectivity in elements, but rather moves the elements while maintaining the connectivity, in order to reduce stress concentration and increase the part's strength.

1.1.1.3.2 Size Optimization

Size optimization often deals with truss-like structures, such as bridges. A typical size optimization problem would involve finding the optimal cross-sectional area for struts. Size optimization can remove elements of the structure if the cross-sectional area is less than a specified value, but it doesn't alter the configuration of members in the structures. Shape and size optimization are concerned with increasing the strength of the part, reducing stress concentration and increasing fatigue life. They do not introduce topological changes in the part, such as adding new holes or voids in continuum structures.

1.1.1.3.3 Topology Optimization

Topology optimization, also referred to as layout optimization, seeks to find the optimal load path for a certain boundary condition, which will allow finding the best material distribution in the part that fulfill certain constraints; such as compliance, displacement, etc. It investigated extensively by Bendsøe and Sigmund in [9].

The optimization assumes that the elements have a relative density, ρ , that varies between 0 and 1 (0 for a void and 1 is for a solid material). This allows for the creation of voids and new holes in the part where needed, unlike size and shape optimization. A typical topology optimization process for continuum structures will generally produce parts that that require shape optimization process in order to reduce stress concentrations (Figure 1-4).

Several approaches have been proposed, which will be discussed in section 2.1.5. The thesis will focus on utilizing the information from this optimization method in the creation of lattice structures, due to its potential in creating optimal material distribution.
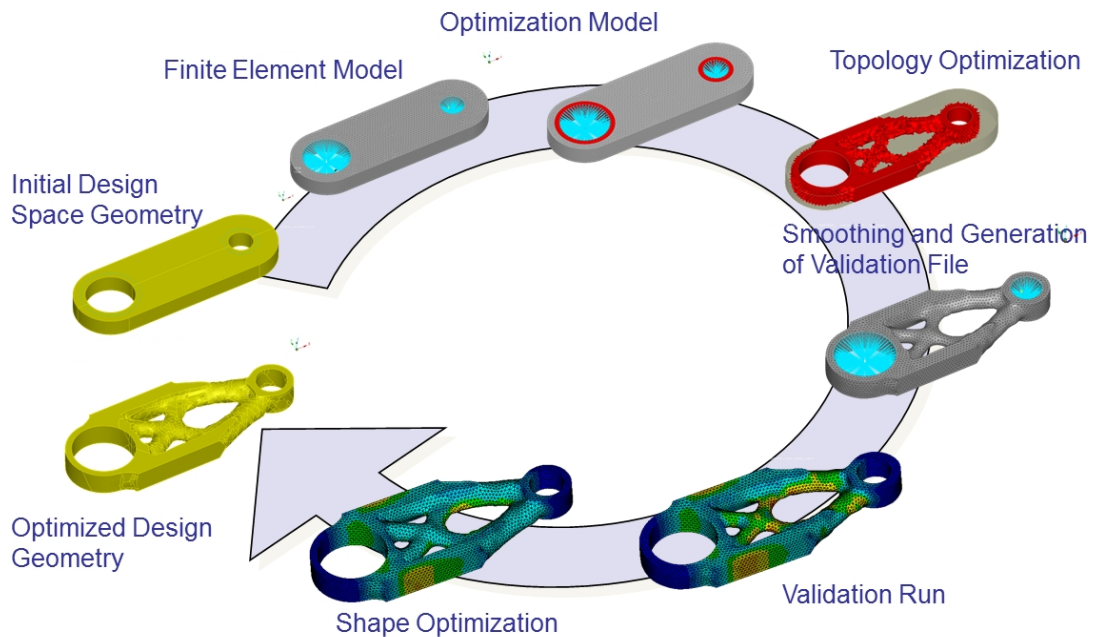
Figure 1-4: Topology optimization workflow [11]

1.1.1.3.4 Topography Optimization

Topography optimization, also known as shell structure optimization, deals with 2-D elements. The main concept is offsetting the elements from the part's mid-plane by varying the spatial coordinates of the nodes as shown in Figure 1-5. The elements' thickness remains constant during the process. This process is useful in sheet metal structures in automotive industry [12] to increase the parts integrity under working load conditions.
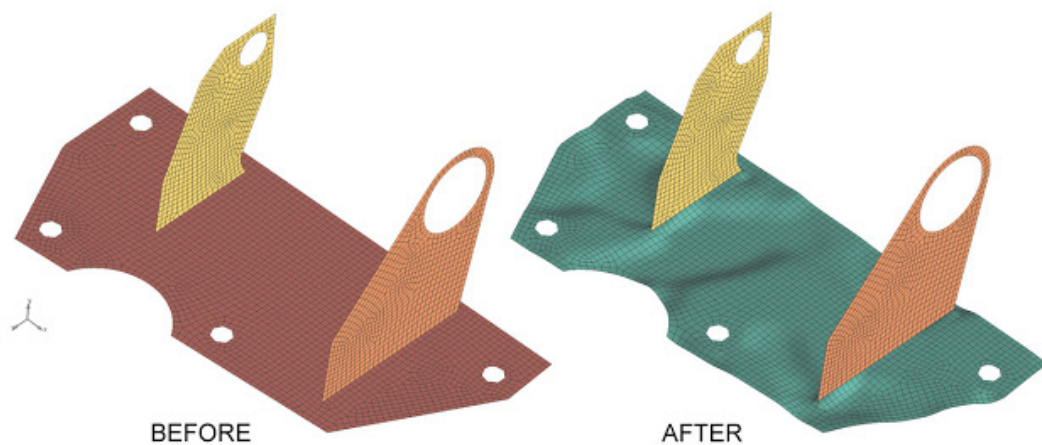
Figure 1-5: Topography optimization [13]

1.1.1.3.5 Topometry Optimization

Similar to topography optimization, topometry optimization deals with 2-D elements but the element offset from the part's mid-plane is not changed, but the thickness of the element as shown in Figure 1-6. This type of optimization is used with parts that are manufactured with AM technology, since it would be difficult and expensive to produce the parts with conventional manufacturing processes.
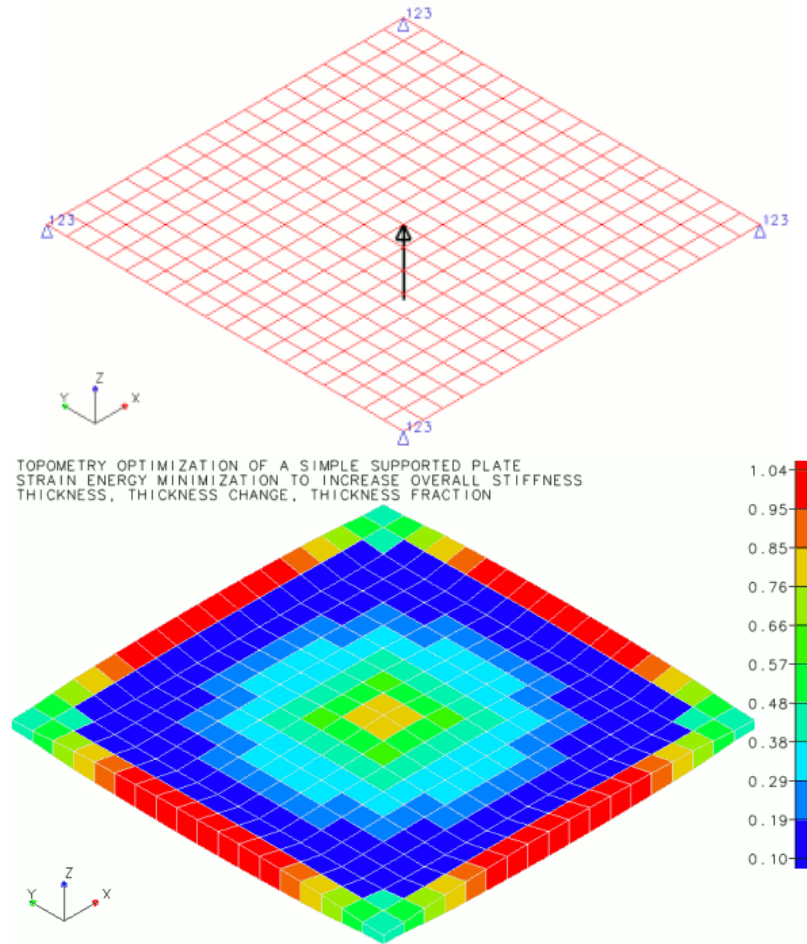
Figure 1-6: Topometry optimization of sheet metal [14]

1.1.2 Motivation

The design of lattice structures can help in creating structures that are both high in stiffness and low in weight. This can be seen in automotive industry, where the complexity of the design of lattice structures arises when the structure contains large number of struts. This would create many local minimums which would pose a problem for optimizing the structure. Also the complexity of the problem is exponentially related to the number of design variables, which would limit the practicality of optimizing such structures.

In the research done by Graf *et al.* [15], an alternative approach, called the Size, Matching, and Scaling (SMS) method, was presented in designing lattice structures by

10

utilizing the information from solid body FEA and a predefined unit-cells configuration (further details in section 2.1.5), which reduced the number of design variables to two and reduced the cost associated with the complexity of the design drastically. The SMS method was then improved by Chang *et al.* [16], to address the limitations in the work done by Graf, such as the lack of other unit-cell configurations. Further improvement was done by Nguyen *et al.* [17] to address other issues such as the ability to generate unit-cells for curved or non-rectangular surfaces.

A major drawback of the SMS method is that it is only applicable to one loading condition. The dependency on the solid body analysis to generate the lattice structure limits the methods performance in structures that are subjected to multiple loading conditions.

1.1.3   Research Questions and Hypothesis

The extensive computational cost associated with the design of lattice structures when the number of variable increases, limits the practicality of the design process.

- **Research question #1:** Can another method for designing lattice structures be developed that eliminates the extensive computational cost associated with the complexity of lattice structures?

The proposed method should not require conducting FEA simulations in order to determine the size of the struts in the generated lattice structure. Using information that is already available that would help guide the designer in where would the optimal material distribution be for the design to handle the applied loads would provide a candidate for developing the method.

- **Hypothesis #1**: By utilizing the relative density information of FEA elements from an already optimized topology model of the design space, the size of the individual struts in the lattice structure can be determined without the need of conducting an optimization process.

To test the first hypothesis, the generated lattice structure's performance using the developed method will be compared with different structures optimized with different methods, including SMS, along with the computational cost (number of FEA simulations) associated with each method.

- **Research question #2:** Can the developed method produce lattice structures that are able to perform reliably against multiple loading conditions?

Since SMS method depends on the stress values from solid body analysis, this will limit its performance to specific loading conditions. Eliminating the dependency on determining the struts' diameter from stress values and utilizing another mean that is not dependent on a single loading condition would accomplish this.

- **Hypothesis #2:** By using an already optimized topology model that is optimized for multiple loading conditions; the information of the relative density of the FEA elements will take into account the different loading conditions, which will improve the generated structure's response to multiple loading conditions.

To validate the second hypothesis, the generated model using the developed method will be tested and compared with the SMS method under two loading conditions.

1.1.4 Organization of the Thesis

Figure 1-7 shows an overview of the topics discussed in each of the following chapters.

Chapter Two - - - - - - - - - - - - ► Literature Review

Chapter Three - - - - - - - - - - - - ► Creation of the Relative Density
Mapping Method (RDM)

Chapter Four - - - - - - - - - - - - ► Example Problems

Chapter Five - - - - - - - - - - - - ► Conclusions and Future work
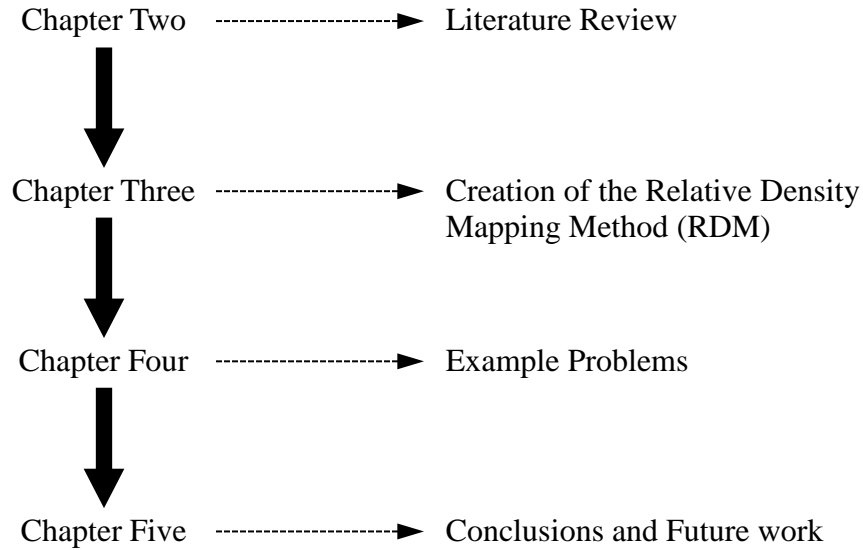
Figure 1-7: Organization of the thesis

Chapter 2 consists of a literature review of the work done in designing lattice structures. This will include different analytical and numerical approaches used to design them. This also includes a literature review of the various methods used in topology optimization. Two optimization algorithms will also be presented in this research.

Chapter 3 will provide details on the development of the method and how density information from topology optimization is utilized in the creation of lattice structures along with a detailed outline of the steps of the design process. Also, an algorithm that will be implemented in MATLAB will be presented in this chapter.

Chapter 4 will provide examples to test and validate the hypotheses made. The first example will show the design process using the proposed method and the effects of changing some of the parameters in the method. The second will show the performance of the method with other methods. The third example will demonstrate the application of the method under two different loading conditions. The fourth example is a practical application of the method in the design of a component of an elevator sling.

The last chapter draws the conclusions limitations of the method and the potential future work in further development of the method.

CHAPTER 2

LITIRATURE REVIEW

2.1 Design of Lattice Structures

2.1.1   Analysis of lattice structures

In designing lattice structures, it is essential to analyze and model these structures to assess their performance. Various researches have been conducted in analyzing cellular structures. Wallach and Gibson [18] have modeled a sheet of lattice structures with a thickness of one unit-cell, which is the building block for the lattice structure. The work was concerned with analytically modeling the elastic properties of the sheet and assumed that the struts of the lattice structure are connected with pin joints, which allows only axial loading on the struts of the lattice structure. The sheet was subjected to axial loading in the x, y and z directions and the results were compared with experimental results giving an error percentage of 3% to 27% depending on the loading direction. Chiras *et al.* [19] focused on similar analysis of the lattice structure sheet under bending and shear loading. Deshpande *et al.* [8] conducted and intensive analysis of the octet-truss lattice structure. The analysis also assumed axially loaded unit-cells to determine the effective mechanical properties of a single unit-cell. By analytically combining these unit-cells, any arbitrary formation is analyzed using an analysis similar to FEA.

Johnston *et al.* [20] analyzed the octet-truss unit-cell with the assumption that the struts behave like beams, which allowed the inclusion of bending, shearing and torsion effects on the structure. The unit-cell was analyzed using a unit-truss model that consists of a central node with set of half-struts connected to it and a common strut between two neighboring unit-trusses. The results had a relative error of less than 10%. Figure 2-1 shows an example of the octet-truss unit-cell and the unit-trusses. Wang *et al.* [21-23]

applied the unit-truss analysis in designing and modeling conformal lattice structures. For the analysis of lattice structures, the FEM will be implemented using the commercial software, ABAQUS.
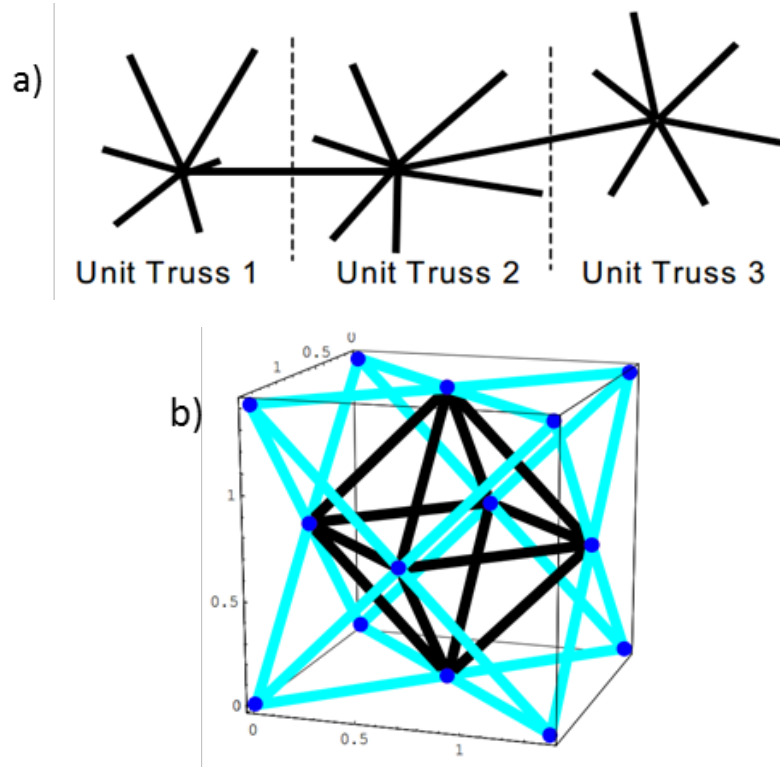
Figure 2-1: a) Three connected unit-trusses b) Octet-truss lattice [20]

2.1.2 Design methods

This section will provide some of the methods used in the design of lattice structures.

2.1.3 Michell's Analytical Approach

In 1904, George Michell theorized the existence of an analytically optimal truss structure for a given load condition [24]. This approach is widely used in the analytical design of truss structures. Many extensions have been made for this approach to include structures that are made from different materials, structures with pre-defined members and non-linear behaviors [25-27]. The approach is restricted in 2-D scenarios, which limits its applicability. Figure 2-2 shows an example of the approach.
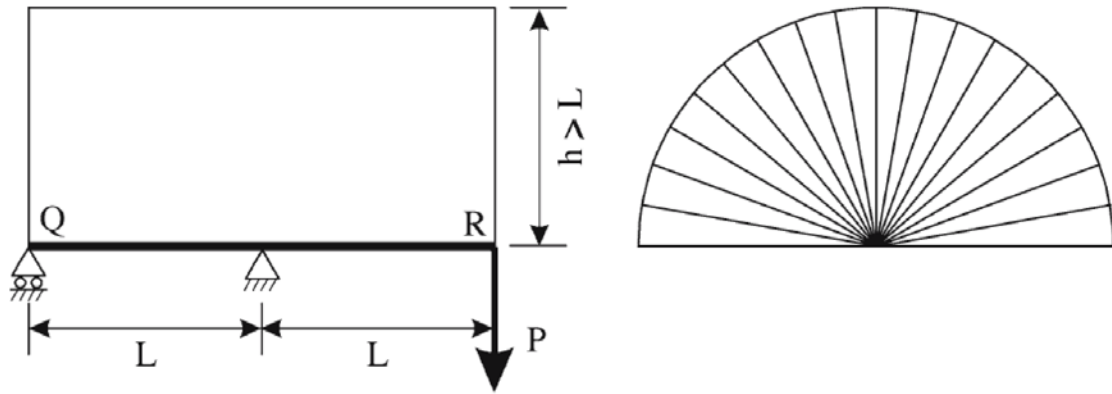
Figure 2-2: A truss designed using the Michell's approach [24]

2.1.4 Optimization approach

Two optimization approaches are used in the design of lattice structures. The ground structure approach and the topology approach.

2.1.4.1 Ground Structure approach

The ground structure optimization approach is a discrete approach used to find the optimal cross-sectional area of the members of a predefined truss configuration that represents all potential connectivity between the structure members [28]. The optimal structure is considered a subset from the initial ground structure. This makes it a size optimization problem with the cross-sectional area of the members as the design variables [29]. However, it can be considered a topology optimization when members are removed from the structure when the size of a member gets small enough [30]. An example of the ground structure approach is shown in Figure 2-3.

Extensions have been made to the ground structure approach to include the position of the nodes of the ground structure as design variables, which makes it also a shape optimization approach [31, 32], and the growth of new members in the structures, such as the Growing Ground Structure Method (GGSM) [33].
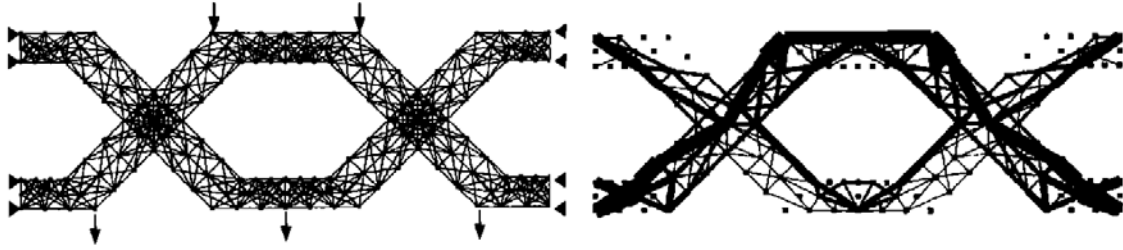
Figure 2-3: Example of ground structure approach [9]

<u>Continuum Topology approach</u>

The topology approach is based on the continuum FEA as described in section 1.1.1.3.3. The advantage of this method is that it can allow changes in the geometry and topology without the need to re-mesh the FEA model [9]. And it is simple to implement the optimization routine [34]. Many researchers believe that the optimal truss structure can be obtained from continuum topology optimization [35].

The draw back in this approach is that ambiguity may arise in interpreting elements which are neither voids ($\rho = 0$) nor solid ($\rho = 1$). This can cause what is known as checkerboard pattern in areas with adjacent low and high relative density elements. Further details on this and the optimization methods used will be presented in section 2.2.

2.1.5 Augmented Size, Matching and Scaling Method

This method was first introduced by Graf *et al.* for the design of lattice structures [15]. It utilizes stress data from solid body FEA results and correlates it to a predefined unit-cell library. However, it lacked a systematic approach in determining the appropriate diameter size for the lattice structure and only had one unit-cell in the library, which is the crossed unit-cell shown in Figure 2-4. Chang *et al.* then addressed those issues in [16] and updated the unit-cell library to include different types of configurations as shown in Figure 2-5. Nguyen *et al.* extended the method so that it can generate conformal lattice structures [17]. Figure 2-6 shows the steps of the method.
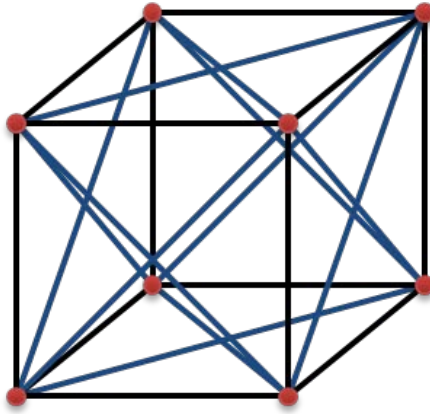
Figure 2-4: Crossed unit-cell structure
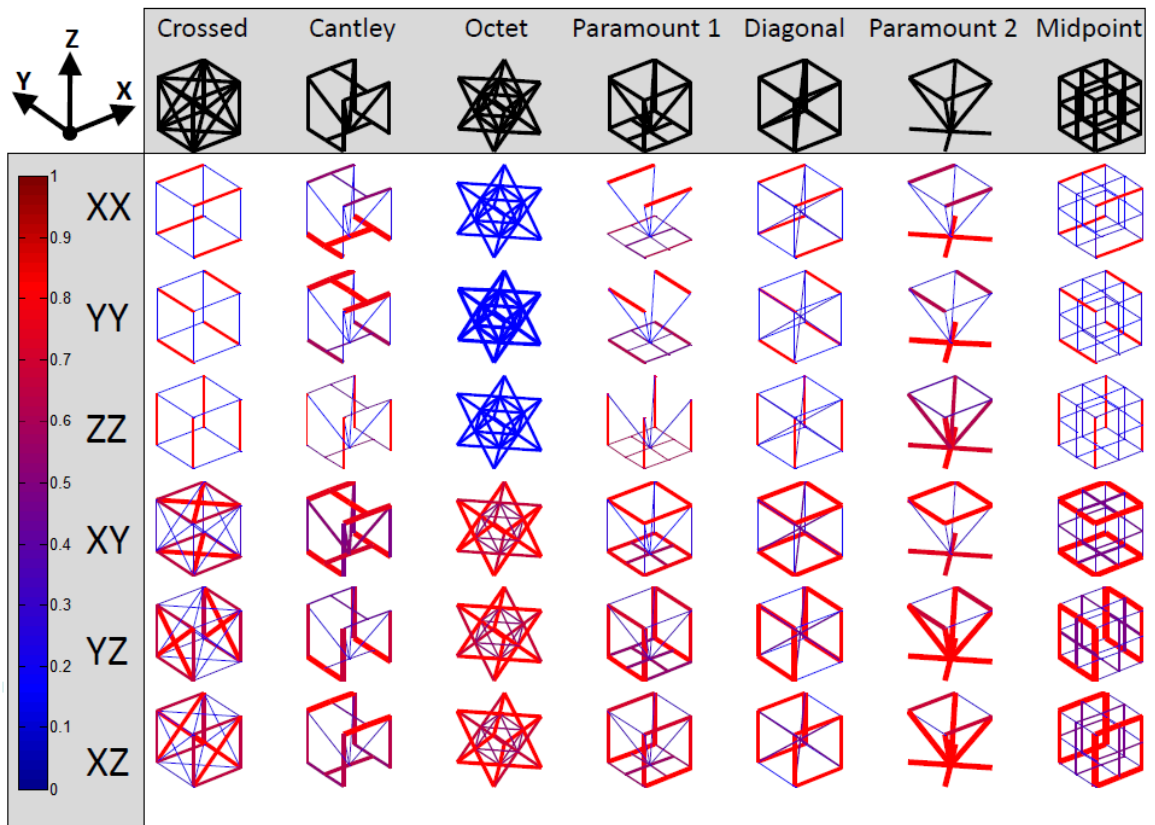
Figure 2-5: Modified unit-cell library [16]
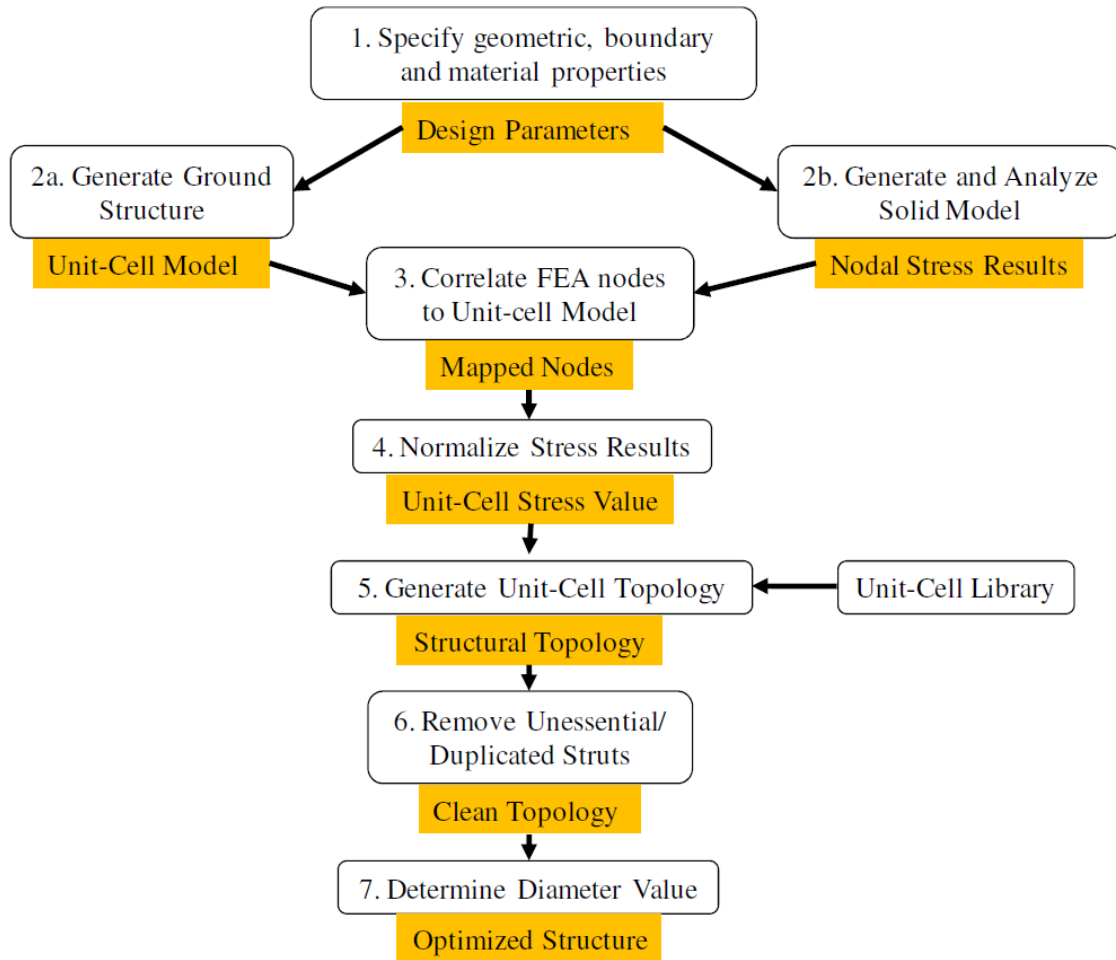
Figure 2-6: Overview of the augmented SMS method [17]

The first step is to prepare the FEA model, which includes the geometry, material, and loading conditions. The second step utilizes the geometry from step 1 to generate the base lattice structure and conducts the FE analysis to obtain the nodal stresses in the model. Then, the FEA nodes are mapped to the base lattice structure to determine which node correlates to which unit-cell region. The extension done by Nguyen utilizes the mesh generated to build the base unit-cells, which eliminates the limitation of the method to simple geometries and generates conformal lattice structures. The obtained FEA stress values are then averaged within a unit-cell and normalized. These stress values are then transformed to the local coordinates of the unit-cell to generate the correct topology from the unit-cell library shown in Figure 2-5. A cleaning process is then performed to remove

duplicate struts, which are overlapping struts generated from two neighboring unit-cells. The last step is determining the minimum and maximum diameters in the structure. This is done by performing an optimization process (using either active-set or Levenberg-Marquardt algorithms) to determine the best values of the diameters.

The dependency of the method on the stress results of the FE analysis limits its generated structures to the specific load case it was designed for.

2.2 Topology Optimization Methods

This section will discuss various topology optimization methods in the literature. The proposed method does not require the topology optimization analysis to be conducted if there is already a topology optimized results of the design problem. In this work however, since the examples provided do not have such results, an optimization process is conducted. The topology optimization will be conducted using ABAQUS/ATOM module.

The target of topology optimization in continuum structures is to find the optimum material distribution in the design space domain Ω in R^2 or R^3. The material distribution domain Ω^{mat} is a subset of the design space Ω (Figure 2-7).
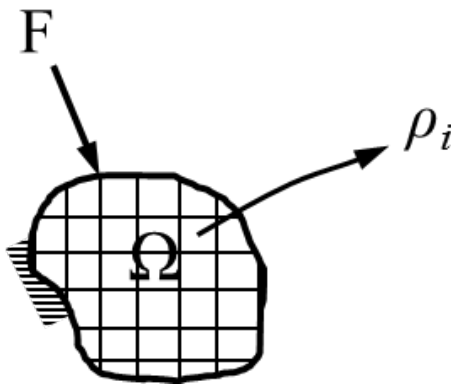
Figure 2-7: Discrete model of the design space with specific load and boundary condition

A typical optimization topology optimization can be formulated as a minimization of strain energy under volume constraints as follows:

20

$$\text{min} \qquad U(\mathbf{\rho}) = \frac{1}{2}\mathbf{u}^T\mathbf{K}\mathbf{u} = \frac{1}{2}\sum_{i=1}^{n}\mathbf{u}_i^T\mathbf{K}_i\mathbf{u}_i$$

$$\text{Subject to} \quad \sum_{i=1}^{n}\rho_i V_i \leq V_0 \qquad\qquad (2\text{-}1)$$

$$0 \leq \rho \leq 1$$

where U is the strain energy, $\mathbf{\rho}$ is the relative density vector, n is the number of finite elements in the model, $\mathbf{u}$ is the global displacement vector, $\mathbf{K}$ is the global stiffness matrix, $\mathbf{u}_i$, $\mathbf{K}_i$, ρ_i and V_i are the displacement vector, stiffness matrix, relative density and volume of element i respectively and V_0 is the desired volume upper bound constraint. Expressing $\mathbf{K}_i$ as a value that depends on the relative density will make ρ_i the design variable of the problem. As seen from equation 2-1, the number of design variables in the optimization depends on the number of finite elements.

Topology optimization methods can be divided into gradient based and non-gradient based optimization methods. In gradient based optimization, the design variables are continuous $(0 \leq \rho \leq 1)$ which allows evaluation of the derivatives of the objective function and then implementing mathematical programming techniques to solve the optimization problem. Examples of these methods are the Solid Isotropic Microstructure with Penalization (SIMP), Rational Approximation of Material Properties (RAMP), and Homogenization Based Optimization (HBO) [36].

Non-gradient based methods have discrete values for the design variables and they are based on repeated evaluation of the objective function using stochastic based algorithms. This allows the design variables to have values of 0 or 1. However, this is difficult to work with mathematically, so the variables are relaxed to allow intermediate values, which makes the function continues and differentiable [37]. These methods include, but are not limited to, Evolutionary Structural Optimization (ESO), Bidirectional ESO, Particle Swarm Optimization (PSO) [38]. These methods are omitted, since most of them are not implemented in commercial software and due to their lack of use in 3-D problems

[36]. Rozvany states that "ESO is presently fully heuristic, computationally rather inefficient, methodologically lacking rationality, occasionally unreliable, with highly chaotic convergence curves" and "ESO is now therefore hardly ever used in industrial applications" [39].

2.2.1 SIMP Method

The basic idea of the method was first introduced by Bendsøe in the late eighties [40]. The name SIMP was given to it by Rozvany *et al*. [41]. The method uses a penalization factor to penalize elements with intermediate densities. The stiffness matrix $\mathbf{K}_i$ depends on the value of the relative density of the element such that:

$$\mathbf{K}_i = \rho_i^P \mathbf{K}_e \qquad (2\text{-}2)$$

where $\mathbf{K}_e$ is the stiffness matrix of a fully solid element, P is the penalization factor. Choosing a value of $P > 1$ will make the intermediate densities unfavorable which allows the generation of relative densities with the values closer to 0 or 1. A values of 3 or more have shown to perform well for both 2-D and 3-D structures [42]. Numerical instability can arise from ill-conditioned stiffness matrix when $\rho = 0$. To avoid this, a lower limit is imposed (e.g $\rho_{\min} = 0.001$). 2-2

The SIMP method is one of the most popularly used because of its simplicity to implement, computational efficiency and the ease to integrate it in commercial FEM software [39].

Some of the drawbacks of the original SIMP method are the generation of checkerboard patterns, entrapment in a local minima and mesh-dependency which are shown in Figure 2-8. Techniques to solve these issues were presented in details in the work done in [37]. Commercial software has normally one or more of these techniques implemented in them.
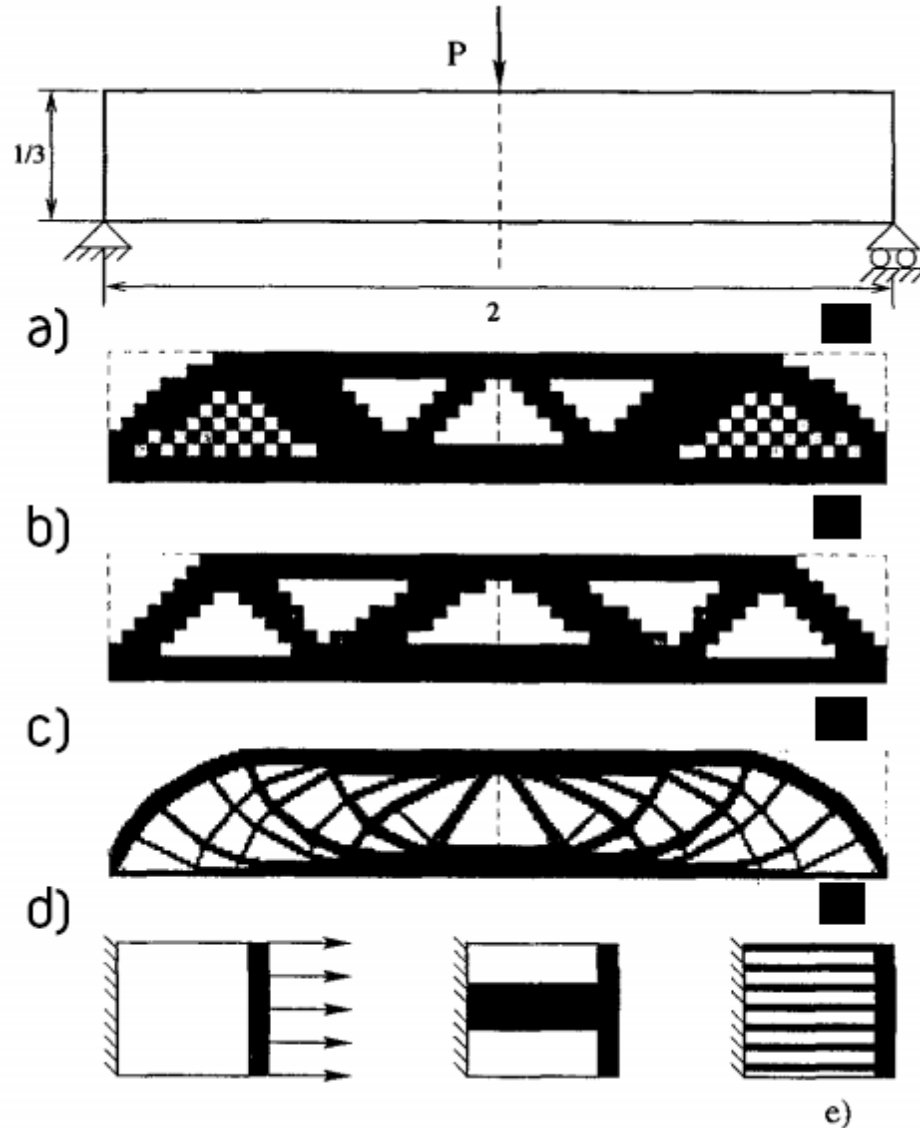
Figure 2-8: Problems that arise in the SIMP method a) Design space b) Checker boarding c) Solution for 600 elements d) Solution for 5400 elements e) Non-uniqueness of solution [37]

Figure 2-9 shows the general work flow of the SIMP method. The model is first prepared by defining the geometry, materials, and loading conditions. The optimization process starts by conducting FEA to evaluate the objective function. Then a sensitivity analysis is conducted by evaluating the derivatives of the objective function. Filtering techniques are then implemented to eliminate checkerboard problems. Then the design variables are updated using an optimization algorithm, such as Method of Moving Asymptotes (MMA) [43]. The optimization loop is repeated until convergence is reached.
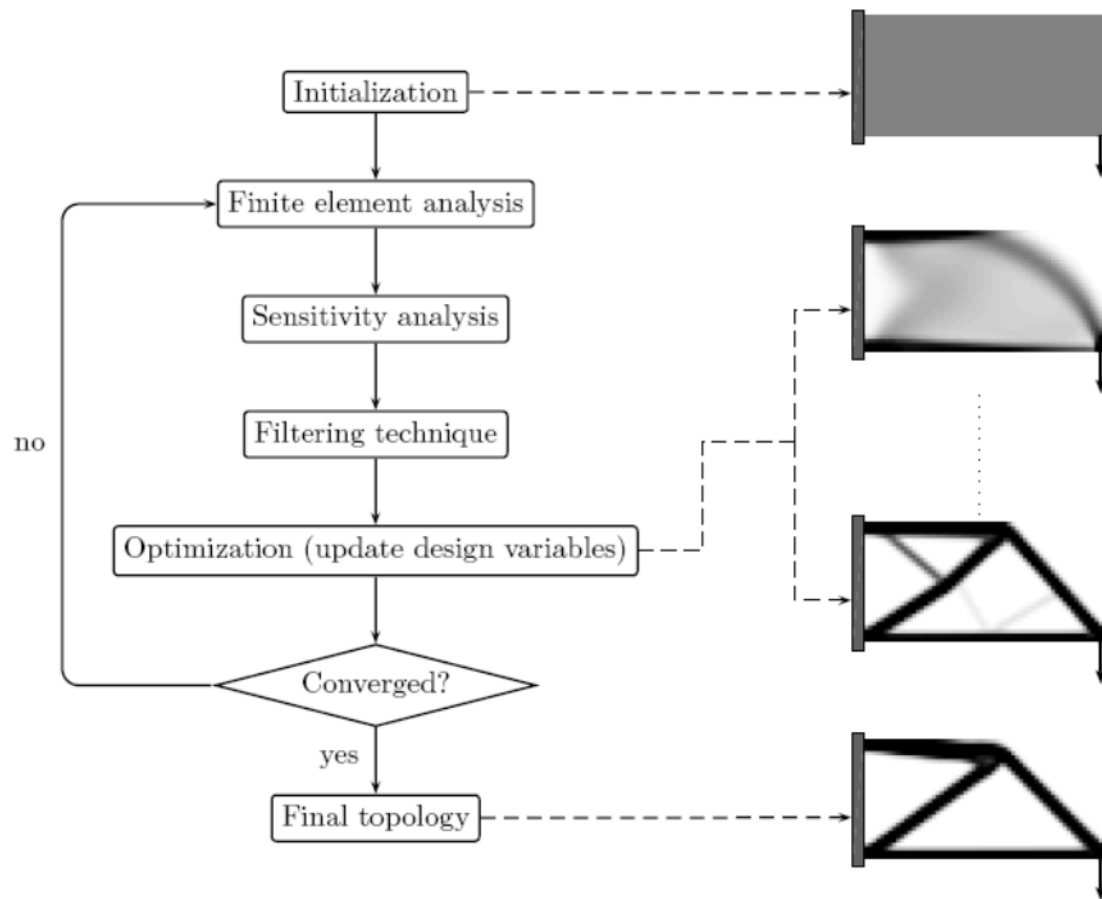
Figure 2-9: Flowchart of the work flow of the SIMP method [44]

2.2.2 RAMP Method

The RAMP method was first introduced in [45]. It was made for problems that have loads that are design dependent, like water pressure on a surface, wind loads, etc. As the problem being optimized, the loaded surface changes and the loads are not unambiguous anymore. A mixed displacement-pressure formulation was then proposed by Sigmund and Clausen [46], which treats the void region as an incompressible hydrostatic fluid that transfers the load to the surface as shown in Figure 2-10. The RAMP method shouldn't be used with problems with concentrated loads. Figure 2-11 show the problem of using it over the SIMP method in a concentrated load problem case.
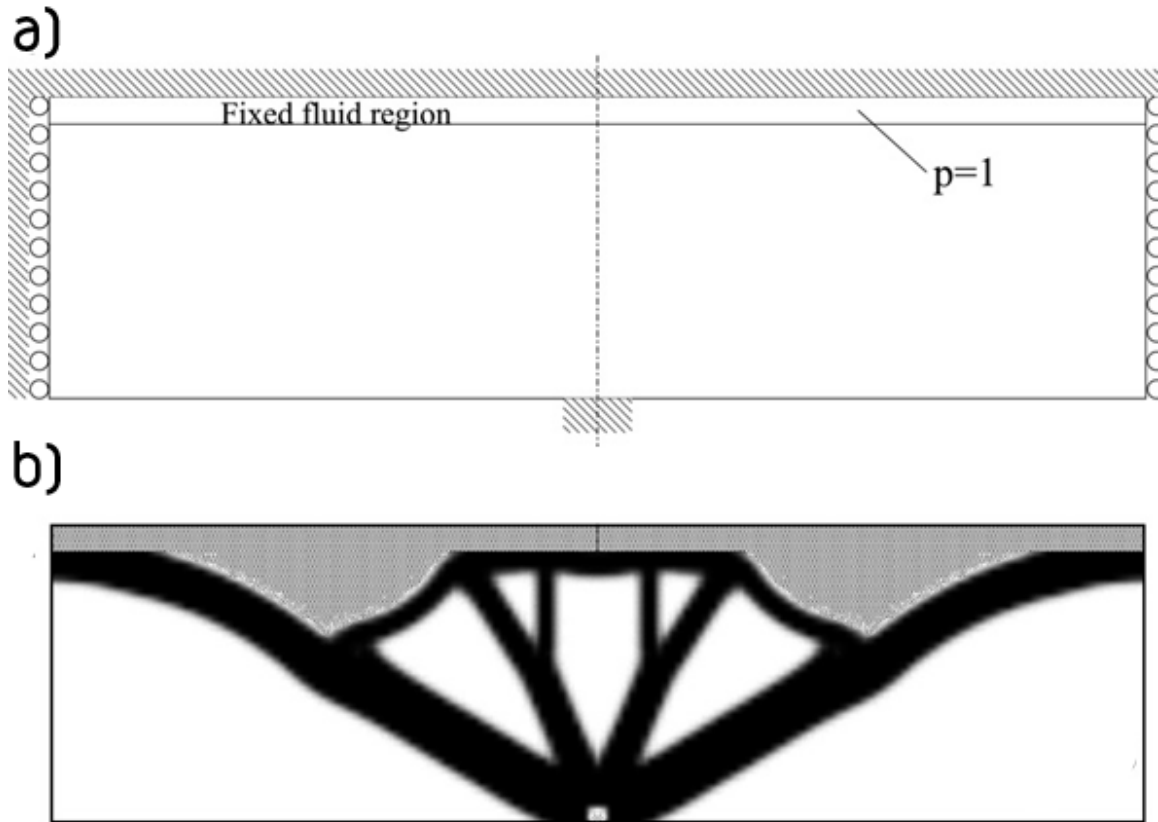
Figure 2-10 RAMP method a) Design space b) Optimized result [36]
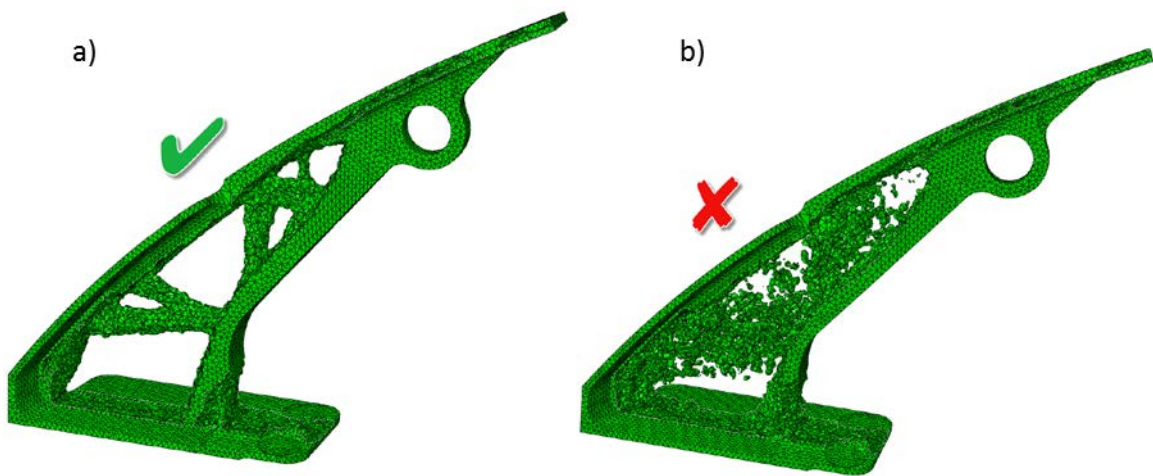
Figure 2-11 Design optimization under concentrated load a) SIMP method b) RAMP method [36]

2.2.3 HBO Method

The HBO was proposed by [47], which uses a composite material representation for the elements, where perforated microstructures called hole-in-cell or layered, as shown in

Figure 2-12, are used. The parameters of these microstructures are the design variables. The stiffness matrix of each element is then numerically calculated by homogenizing the properties of the microstructure. A point on the structure can be fully occupied with material ($\rho = 1$), a void ($\rho = 0$) or partially occupied ($0 < \rho < 1$), which is a porous composite at micro level.
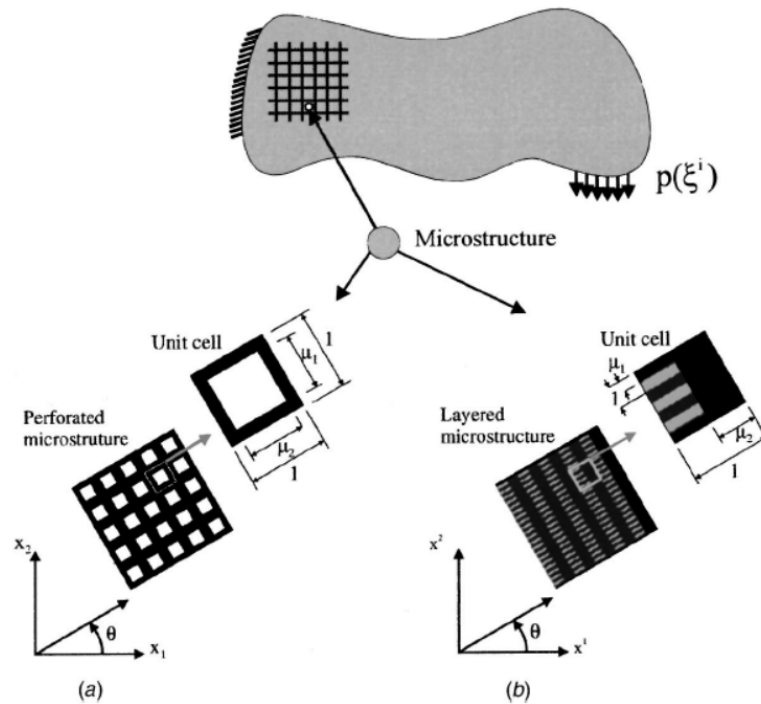
Figure 2-12 HBO microstructures a) Hole in cell microstructure b) Layered microstructure

2.3 Multi-variable optimization algorithms

Every optimization method will require an actual optimization algorithm to be used to be used. The work done on the SMS method by Chang utilized two algorithms; the active-set and Levenberg-Marquardt (LM) algorithm. The two algorithms will be discussed in this section. These algorithms will also be implemented in the ground structure approach in CHAPTER 4 for evaluating the performance of the proposed method.

2.3.1 Active-Set Algorithm

Active-set is a mathematical programming algorithm that uses gradient for optimizing bound large scale problems [48]. The algorithm, as the name suggest, determines which inequality constrain in a set of constraints in a given minimization will influence the final optimization results. These constraints are called the working set. One constraint may be added or deleted from the working set in each iteration. This will help in reducing the time and complexity of the optimization. In MATLAB, the function *fmincon* will be used to implement the active-set algorithm, which is coupled with Sequential Quadratic Programing methods (SQP) [49].

2.3.2 Levenberg-Marquardt (LM)

Levenberg-Marquardt is an optimization algorithm that is a gradient based that is most used for non-linear least square minimization problems. The target values are formulated as a regression problem by squaring the error between the actual and target values. The limitation of this method is in the increased computational effort with the increase in number of variables [50]. The MATLAB function *lsqnonlin*, which is a non-linear least square solver, is used [51].

2.3.3 Summary

A literature survey was conducted and presented in this chapter. The survey included the analysis and design of lattice structures using different design methods, such as Michell's analytical method, optimization approaches (ground structure and topology optimization), and the augmented SMS method. A survey of different methods used in topology optimization was presented along with multi-variable optimization algorithms that will be used in this research.

CHAPTER 3

RELATIVE DENSITY MAPPING METHOD (RDM)

This chapter will explain the basic idea of the formulation of the Relative Density Method (RDM) and a detailed overview of the process of generating lattice structures using this method.

3.1 Formulation of the RDM Method

As the name of the method suggest, it uses the relative density information that were obtained from a topology optimization process in order to generate lattice structures. Figure 3-1 shows a 2-D example of a strut, j, surrounded by elements with different relative density values. The key idea of RDM is that, a strut that is surrounded with elements with high relative density values will have higher relative cross-sectional area value compared to a strut surrounded with elements of low relative density.
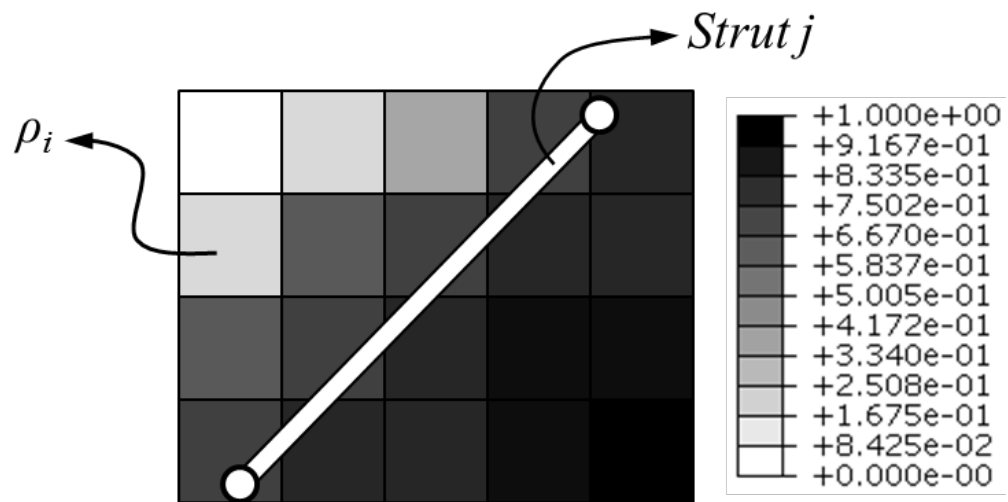
Figure 3-1: Relative density mapping to strut diameter

To formulate a mathematical relation between the relative densities and strut's cross-sectional area, the following conditions were set:

28

- Elements that are closer to the strut will influence its relative cross-sectional area more than those who are far from the strut.

- The relative cross-section value of the strut must depend on the average influence of the relative densities of all elements.

- The upper value of the strut's relative cross-sectional area is 1.

From the first two conditions, it is clear that a weighted average of the relative densities would be an appropriate formulation, where the weights are functions that depend on the distance of the element from the strut

$$Ar_j = \sum_{i=1}^{n} \frac{\rho_i w(r_{ij})}{w(r_{ij})} \tag{3-1}$$

where Ar_j is the relative cross-sectional area of strut j, w is a weight function and r_{ij} is the distance of element i from strut j. The third condition acts as a limiting value for the relative cross-section of the strut. Since ρ_i has a maximum value of 1, then w should also have a maximum value of 1 when the distance between the element and the strut is 0. And should decay as the elements get further away from the strut. To achieve this, an exponentially decaying function is used.

$$w(r_{ij}) = \exp(-r_{ij}) \tag{3-2}$$

To calculate the distance of each element from the strut, the coordinates of the elements' centroidal coordinates are calculated. Then, the strut is treated as a line segment with length L to find shortest distance between it and the elements' centroids and the line segment. Figure 3-2 shows an illustration of this.
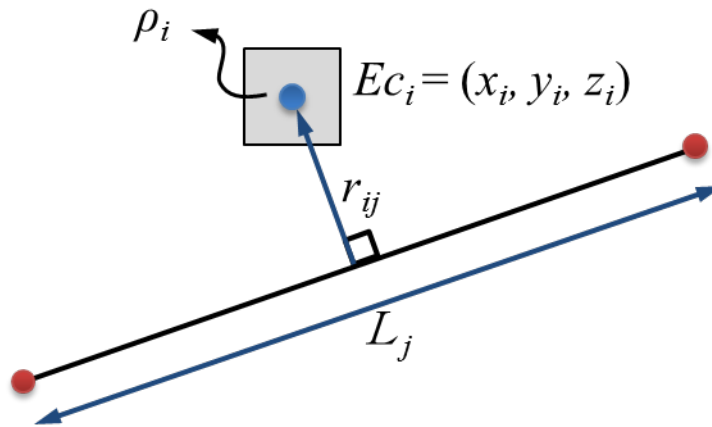
Figure 3-2: Illustration of the distance of the centroid of element *i* from strut *j*

The values of the elements' centroidal coordinates are stored in an array **Ec**. For each strut, the shortest distance from it and from each entry in **Ec** is calculated and stored in the distance array **r**.

3.2 Overview of the Process of Generating Optimized Lattice Structures

This section will present a detailed explanation of the process used to generate the optimized lattice structures. The process can be divided into five major steps. Each step (rounded rectangle) will produce an output (shaded box) which will serve as an input to the next step. Each step in the process will be explained in the following format:

- **Step description:** Explanation of the step.
- **Deliverables:** The primary deliverables of the step.
- **Additional Information:** Any other information or assumptions used in the step.
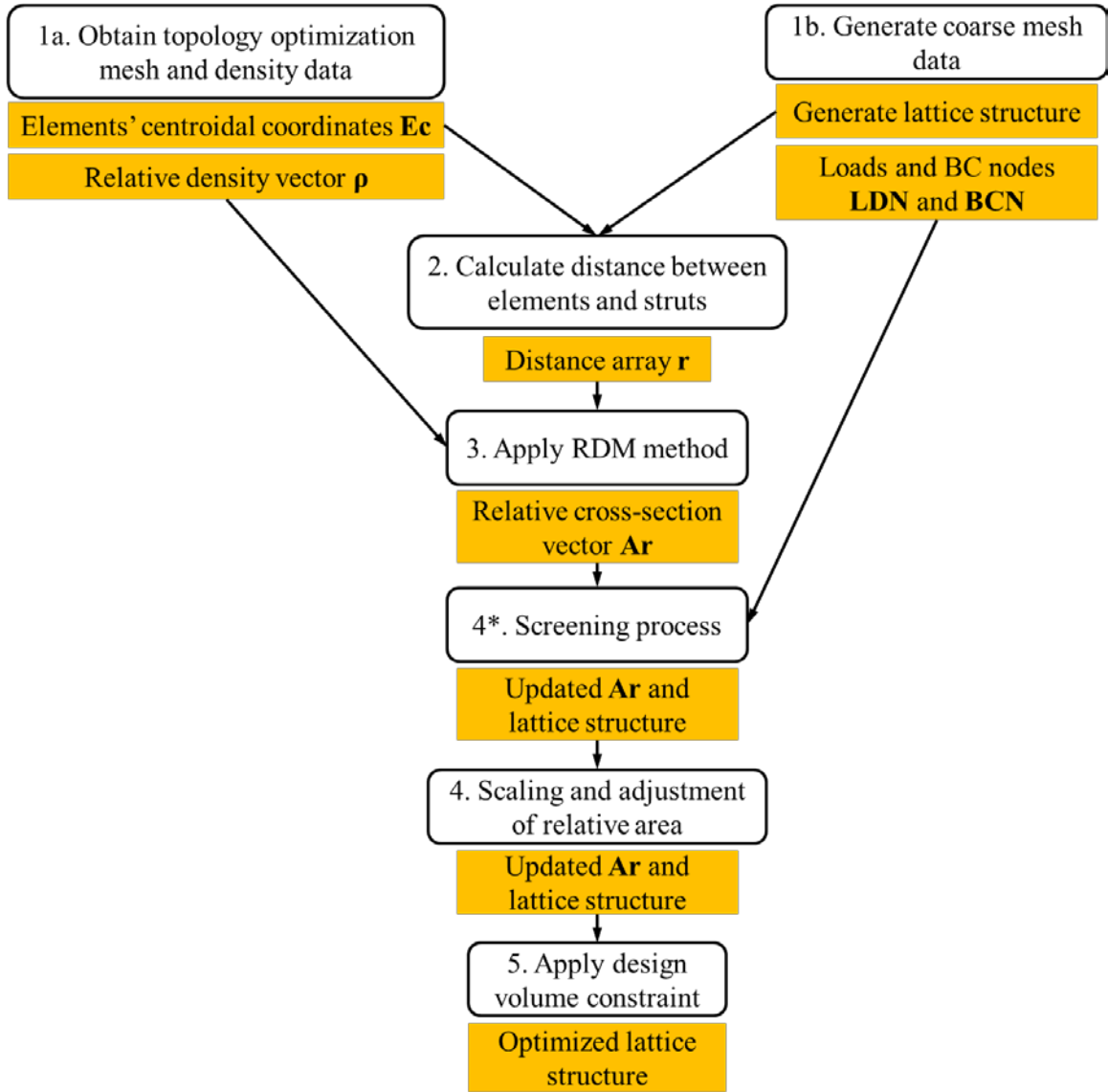
Figure 3-3: Overview of the process for generating optimized lattice structure

3.2.1 Step 1a: Obtaining the Topology Optimization Mesh and Density Data

3.2.1.1 Step Description

In this step, the required input is the information obtained from the topology optimization process and the data of the FE mesh. From the topology optimization process, the relative density values are extracted. From the FE mesh data, the nodal coordinates and the connectivity nodes of each element are extracted. The values of the relative density will

be used in equation 3-1 for the determination of *Ar* values. The nodal coordinates will be used along with the connectivity nodes of each element to calculate the element's centroidal coordinates *Ec*, which will be used in the calculations of the distance between the elements and the desired strut.

<u>3.2.1.2   Deliverables</u>

The primary deliverables of this step are centroidal array **Ec**, that contains the coordinates of all the centroids of the elements used in the topology optimization process, and the vector $\boldsymbol{\rho}$ that contains the relative density values of all elements. The values of **Ec** will be used as input to step 2, while $\boldsymbol{\rho}$ will be used as input for step 3.

<u>3.2.1.3   Additional information</u>

It is assumed in this process that the results of the topology optimization are already available for the designer. In this research however as stated before, there were no already available results for the cases used in the examples. So the topology optimization process was conducted to obtain the required inputs.

3.2.2   Step 1b: Generating Coarse Mesh Data

<u>3.2.2.1   Description</u>

In this step, a FE model of the required design space is generated but with a coarser mesh, which includes the nodes, elements' connectivity, loads, and boundary condition nodes. The generated elements will be used as the base structure to create the crossed unit-cells shown in Figure 3-4. This will enable the generation of lattice structures that are conformal to the surface of the design region. The load and boundary condition nodes will be used as an input for step 4* if required.
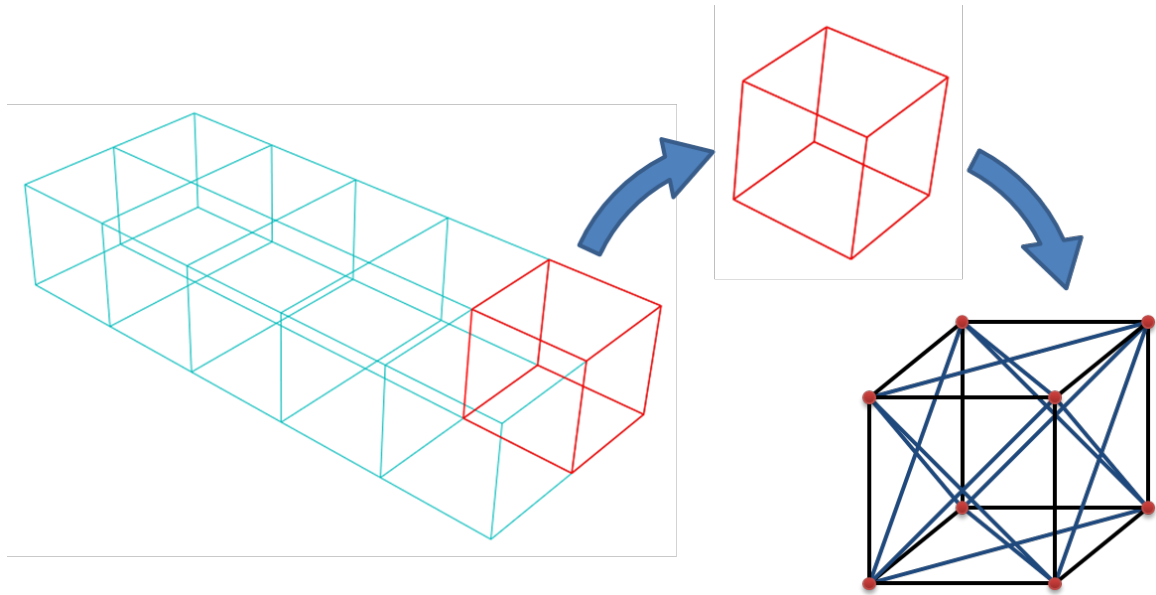
Figure 3-4: Generating unit-cells using FE mesh

Deliverables

The deliverables from this step are the generated lattice structure and the information obtained from it. This information includes the length of each strut in the generated unit-cell, L (which will be stored in a vector array **L**), the connectivity nodes of each strut, the nodal coordinates of these nodes and also an array of the nodes that are subjected to loads, **LDN**, and boundary conditions, **BCN**.

3.2.2.3 Additional information

The use of a coarse mesh in this step allows the struts to be surrounded with as many elements from the topology optimization as possible. If the same element size as the topology optimization mesh is used, the struts will be weakly influenced by the surrounding elements, since their centroids will be far from the struts. Duplicate struts (struts that share the same nodes) are eliminated in this step so that only one of the struts remains. The generated struts are created as linear beam elements (B31).

3.2.3   Step 2: Calculating the Distance between Elements and Struts

3.2.3.1   Description

By using the values of **Ec** and the information obtained from step 1b, the distance of each element from each strut are calculated in this step.

3.2.3.2   Deliverables

The output of this step is an array, **r**, which contains the distance of all elements' centroids from each strut. The columns of the array contain the distance of the elements centroids from a specific strut.

3.2.3.3   Additional Information

When calculating the distance, the struts are treated as a line segment (not an infinite line) and the shortest distance is then calculated accordingly.

3.2.4   Step 3: Applying the RDM Method

3.2.4.1   Description

This step will determine the relative cross-sectional areas of the struts by using the values of ρ and **r** obtained from steps 1a and 2 respectively. These values will be implemented in equations 3-1 and 3-2.

3.2.4.2   Deliverables

For this step, the primary deliverable is the vector **Ar**, which contains the values of the relative cross-sections of all struts. The next steps will provide a form of treatment to these values according to their objective.

3.2.4.3   Additional information

Some of the generated values of *Ar* can be extremely small. This may cause some issues later on so they will be treated in the next steps.

3.2.5   Step 4*: Screening Process (Optional)

3.2.5.1   Description

This step is an optional step. It is used to eliminate any structurally unessential struts that have no effect or contribution on the over-all performance of the lattice structure, and struts that have small values of *Ar* relative to a certain rejection ratio value, *RR*. Therefore, these struts can be removed to increase the performance of the lattice structure. The flowchart for removing these struts is shown in Figure 3-5.

The process starts by first determining the nodes that are contained in **LDN**. The FE elements that are associated with these nodes are fixed and won't be removed with the screening process. Elements that are totally fixed are removed from the structure. These elements can be identified by checking if all their nodes are all contained in **BCN**. After determining the load and BC elements, a rejection ratio value is set. All elements that have values of *Ar < RR* are removed from the structure. This can help in increasing the structure's performance by removing small sized struts.

After the removal process, some elements may remain that have no benefit on the structures performance. An example of these elements is shown in Figure 3-6. To determine these elements, an iterative process is conducted. The iteration assumes that the struts are pin connected. It starts by removing all elements that have a free node. A free node is a node that is connected only to one element (these node appear after the removal of elements with *Ar < RR*). After the removal of these elements, another check-up is conducted. This check-up scans the structure for any nodes that have only two

elements connected to it. If these elements are connected by a 3rd common element, then the elements that are connected to that node are removed. Otherwise, they are left alone.
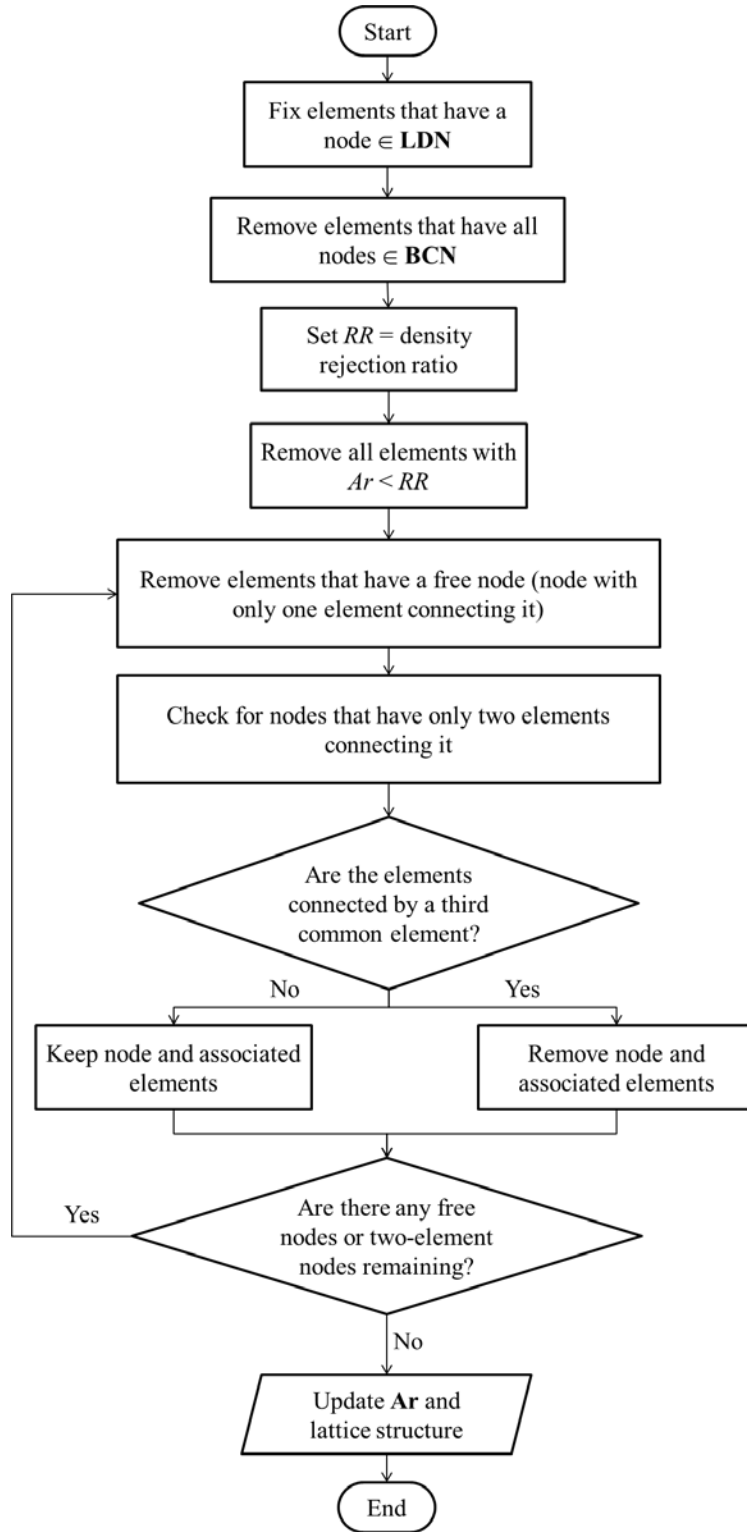
Figure 3-5: Flowchart of the screening process

After this process, the iteration loops back and checks again for free nodes or two-element nodes. If no such nodes remain in the structure, then the iteration stops and the structure and relative area are updated. Figure 3-6 a) shows that after the first removal iteration, a node becomes an unwanted node. The assumption of pin connected nodes would render the struts connected to that node useless. But if the nodes are rigid connections, these struts would affect in the stiffness of the structure. But the removal of these struts would allow more materials to be added to the remaining struts which would make the structure stiffer than if they were left. So the assumption of pin connections will not reduce the performance of the generated structure.
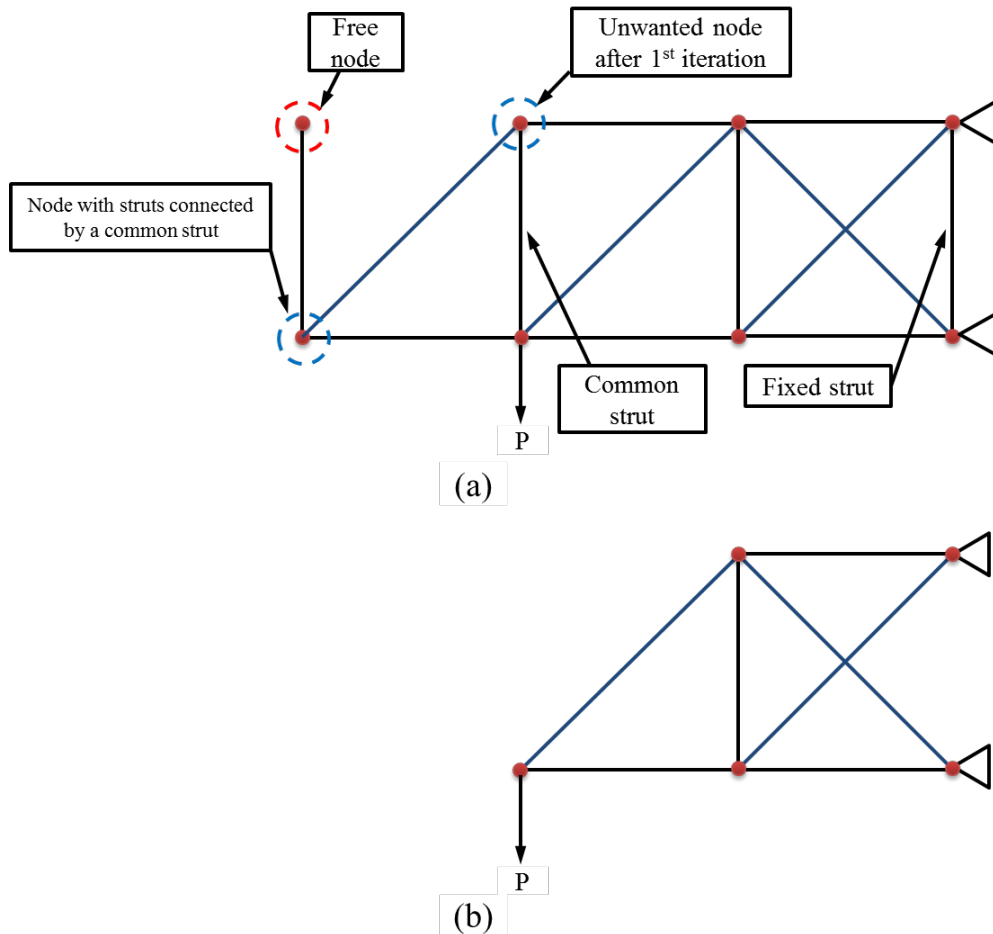
Figure 3-6: a) Initial structure before the screening process b) Structure after screening process

As stated, this step is an optional step. The reason being is that it can produce structures that have essential struts removed. This can happen when the value of *RR* is high. Also, the removal of the free node and two-element node elements does not remove all unessential elements in the 3-D case and may not work properly if other unit-cells were to be implemented in future work.

3.2.6   Step 4: Scaling and Adjusting the Lower Relative Area Values

3.2.6.1   Description

Since the minimum value of ρ is ρ_{min} (e.g. 0.001); when generating the values of *Ar*, some of them will be extremely small. This can cause numerical instability problems of ill-conditioned stiffness matrices for the beam elements used. To avoid this issue the values in **Ar** are adjusted and scaled so that

$$\min(\mathbf{Ar}) = Ar_l$$
$$\max(\mathbf{Ar}) = 1$$
(3-3)

where Ar_l is a lower limit for the values in **Ar**. This is somewhat similar to the diameter ratios done by Graf [52], where the ratio will be Ar_l, but this process is done before generating the physical diameters of the struts. Applying the screening process will also help in eliminating this problem. But the values of Ar_l can affect the overall performance of the structure as it will be discussed in CHAPTER 3.

The process is done so that the ratio between any two differences between the relative areas remains the same after the adjustment. This scaling and adjustment of the values is done as follows:

$$Ar = \underbrace{\left[\frac{1 - Ar_l}{\max(\mathbf{Ar}) - \min(\mathbf{Ar})} \right]}_{\text{Scaling part}} \times \underbrace{\left[Ar - \max(\mathbf{Ar}) \right] + 1}_{\text{Adjustment part}}$$
(3-4)

After the scaling and adjusting process is done, the generated output of this process is a modified **Ar** vector with values between Ar_l and one. This output will be used in the next step to generate the final optimized lattice structure.

3.2.6.3 Additional Information

The selection of the value of Ar_l will affect the performance of the final structure. From the observations of different tests, the value of Ar_l that produces the optimal structure is relatively small. An optimization process may be used in future work to determine the optimum value for Ar_l.

3.2.7 Step 5: Apply Design Volume Constraint

3.2.7.1 Description

This is the last step in the design process of the lattice structure using RDM method. In this step, the required volumetric design constraint, V_0, is applied. This is done by scaling the **Ar** vector so that the total volume of the structure is the same as the volume constraint. The scaling factor can be calculated as follows

$$Sf = \frac{V_0}{\sum_{j=1}^{N} Ar_j \times L_j} \tag{3-5}$$

Where Sf is the scaling factor and N is the total number of struts in the structure. Then Ar is updated by multiplying it with Sf

$$\mathbf{Ar} = Sf \cdot \mathbf{Ar} \tag{3-6}$$

3.2.7.2   Deliverables

From this step, the output is the final optimized lattice structure with the appropriate scaled cross-sectional areas.

3.2.7.3   Additional Information

The diameters of each strut are obtained from the cross-sectional area values. It should be noted that there is no constraint on the stresses on the generated design, which is a drawback that will be addressed in future work for the method.

3.3 Algorithm to Implement RDM Method

In this section, an algorithm to implement the RDM method will be outlined which will summarize the five steps that were explained section 3.2. This algorithm will be used to write a MATLAB code to generate the optimized lattice structure. The algorithm is as follows:

1. Input topology optimization relative density ρ and FEM mesh data (nodal coordinates, mesh node connectivity).
2. Input coarse FEM mesh data (nodal coordinates, mesh node connectivity).
3. Set number of elements in topology FEM data to n and calculate elements' centroidal coordinate vector **Ec**.
4. Generate unit-cells from coarse FEM input data and set number of struts to N.
5. Start loop to calculate relative cross-section area, **Ar**. (Set $j = 1$)
   5.1. Select strut j.
   5.2. Calculate the distance of all elements in **Ec** from strut j and store them in $\mathbf{r}_j$.
   5.3. Calculate the relative cross sectional area Ar for strut j using ρ, $\mathbf{r}_j$.
   5.4. Repeat 6.1 until $j = N$.
6. Opt to apply screening process.
7. Set Ar_l value.
8. Adjust and scale **Ar**.
9. Calculate Sf.
10. Scale **Ar**.
11. Generate optimized lattice structure.

Figure 3-7 shows the flowchart for the RDM method.
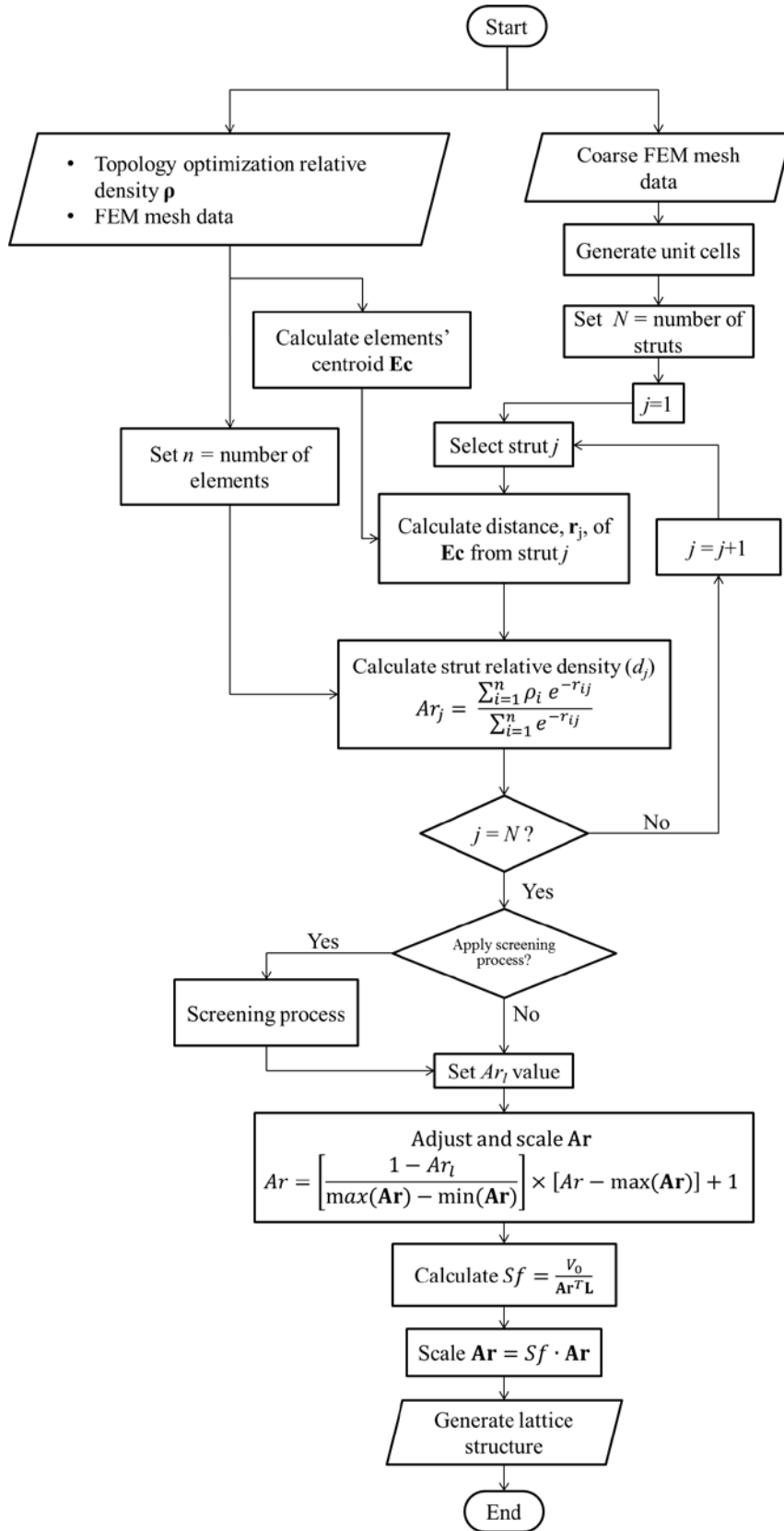
Figure 3-7: RDM method flowchart

3.4 Summary

This chapter presented the formulation of the RDM method and the basic idea behind it. It also provided a detailed step by step overview of the process of generating lattice structures using RDM. The process starts with the data from topology optimization results, which will be used to calculate the struts' relative cross-sectional area using RDM method. A scaling and adjustment process is then performed to set a lower limit for the minimum relative cross-section. Then the structure's diameters are scaled according to the volumetric design parameter. The structure can be cleaned from unwanted struts before the scaling and adjusting of relative cross-sectional area process. An algorithm was also provided in this chapter that was used to create a MATLAB code to generate the lattice structure.

CHAPTER 4

DESIGN EXAMPLES

This chapter will present examples of the application of the RDM method on designing lattice structures. The first example will discuss the application of RDM on a 2-D cantilevered beam and show the effects of different unit-cell sizes and the values of Ar_l and RR on the performance of the design. The second example will compare the performance of RDM with SMS and ground structure in designing 3-D curved cantilevered beam. This will also show how the methods are used in generating conformal lattice structures. The third example will show the advantage of RDM over SMS in designing a 3-D beam that is subjected to multiple loading conditions. The last example is the application of the method in the design of an elevator component using RDM. The example will show the advantage of the method in designing light-weight and stiff component for industrial applications.

4.1 2-D Beam Design Using RDM

4.1.1   Problem Description

In this example, the design process using RDM method will be presented. Effects of the value of Ar_l and RR will be discussed in this section along with the assumptions that will be carried on for the design examples in the following examples.

The example used is similar to the one in [9]. The example is of a cantilevered beam with a load in the middle of the tip of the beam. The properties of the beam are shown in Table 4-1. The characteristic dimensions of the beam allow it to be translated to a 2-D problem. Figure 4-1 shows the cantilevered beam and the results of the topology optimization of minimizing the strain energy at 20% volume fraction constraint, which is similar to the result in [9].

Table 4-1: 2-D Cantilevered beam properties

Length (mm)	40
Height (mm)	10
Thickness (mm)	1
Loading magnitude (N)	1
Modulus of Elasticity (MPa)	1960
Unit-cell size in-plane (mm)	5
Unit-cell size out-plane (mm)	5
Target volume (mm^3)	80
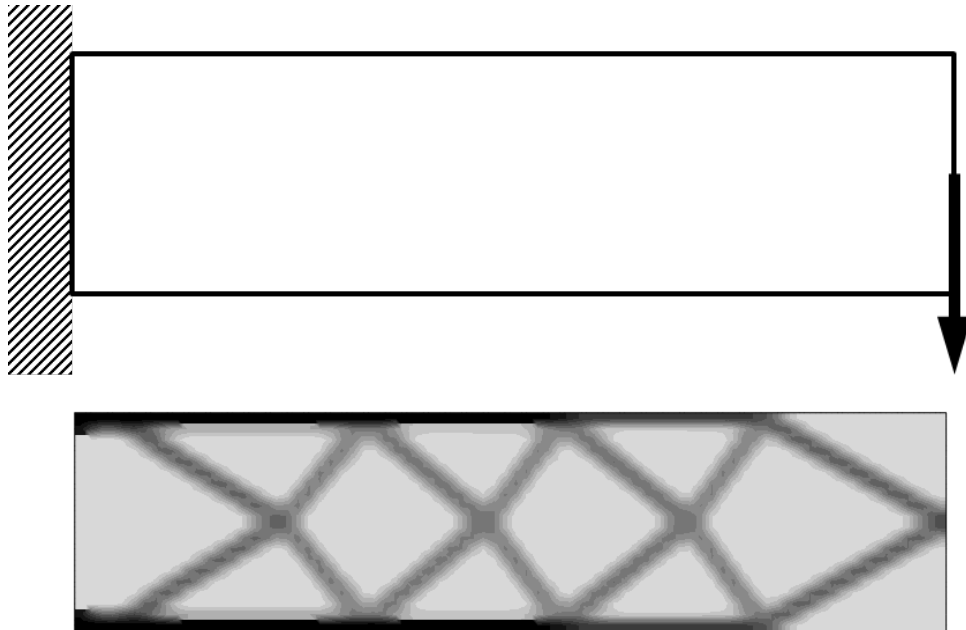
Figure 4-1: Cantilever beam example

4.1.2   Generating the Lattice structure

The design process starts by generating a coarse mesh that will act as the base for generating the unit-cells. A size of 5×5 mm is used for the mesh as shown in Figure 4-2.

a)

b)
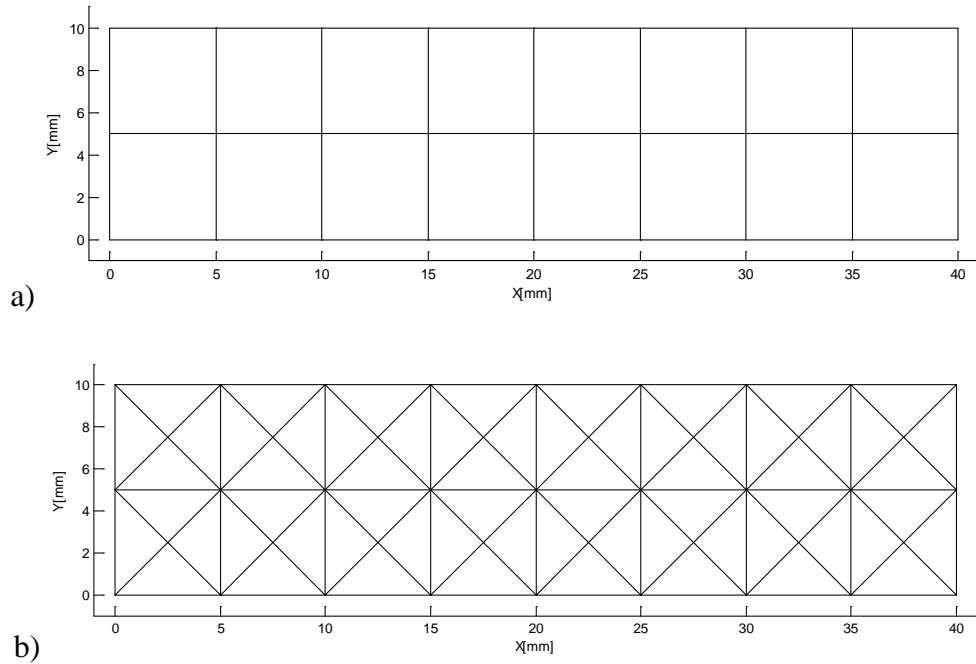
Figure 4-2: a) Coarse FEM mesh b) Generated unit-cell struts

The data of topology optimization and the generated lattice structure are then implemented in the MATLAB code to estimate the cross-sectional area of each strut with values of $V_0 = 0.2$, $Ar_l = 0.001$ and $RR = 0$ (no screening process). Figure 4-3 shows the generated lattice structure. As seen in the figure, the struts where there are large bending stresses are larger.
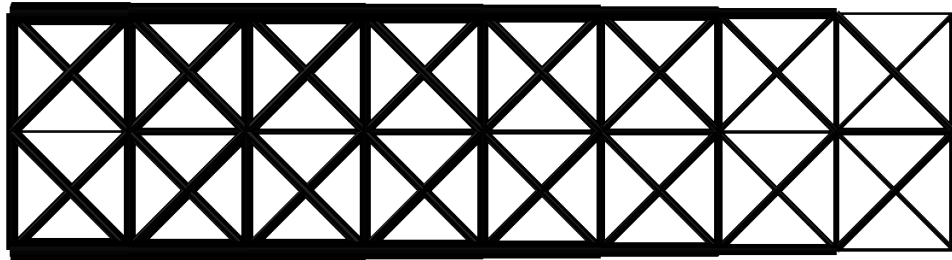
Figure 4-3: Generated optimized lattice structure using RDM

4.1.3   Process Results

The beam had a deflection at the loaded point of 0.49mm, which is less than a structure with equally sized struts, which had a deflection of 1.14mm. Both Active-Set and LM

algorithms were implemented on how well the process optimized the structure with the following formulation:

$$\min Z(\mathbf{D}) = \sum_{j=1}^{N} \left[\left(w_d \times \delta(D_j)\right)^2 + \left(w_v \times \frac{V(D_j) - V_0}{V_0}\right)^2 \right] \qquad (4\text{-}1)$$

Where w_d and w_v are weight variables of values of 1 and 100 for the deformation and volume respectively, δ is the deformation of the structure and V is the volume of the structure. Both δ and V are functions of the individual struts' diameters $\mathbf{D}$. For active-set optimization, the upper and lower bounds of the struts' diameters are the constraints. Table 4-2 shows the results of the optimization process. Active-set had the least displacement of the tip but required more simulations than LM. The displacement obtained with RDM is higher than the ones obtained by active-set and LM but would require no FE simulations if the topology optimization results are present. If the results are not available, the method required 55 FE simulations.

Table 4-2: Optimization results for 2-D beam

Method	Tip displacement (mm)	No. of Simulations	
Identically sized structure	1.14	-	
Ground structure (Active-set)	0.1447	7407	
Ground structure (LM)	0.3657	3402	
RDM ($Ar_l = 0.001$)	0.48	-	55

4.1.4 Base Unit-cell Size Effect

To check if the size of the unit cell affects the performance of the structure, two other sizes were investigated, 2.5×2.5 mm and 5×10 mm. Figure 4-4 shows the generated lattice structures using these sizes. The generated structures were optimized using RDM (Figure 4-5), and the results of the optimization are shown in Table 4-3.
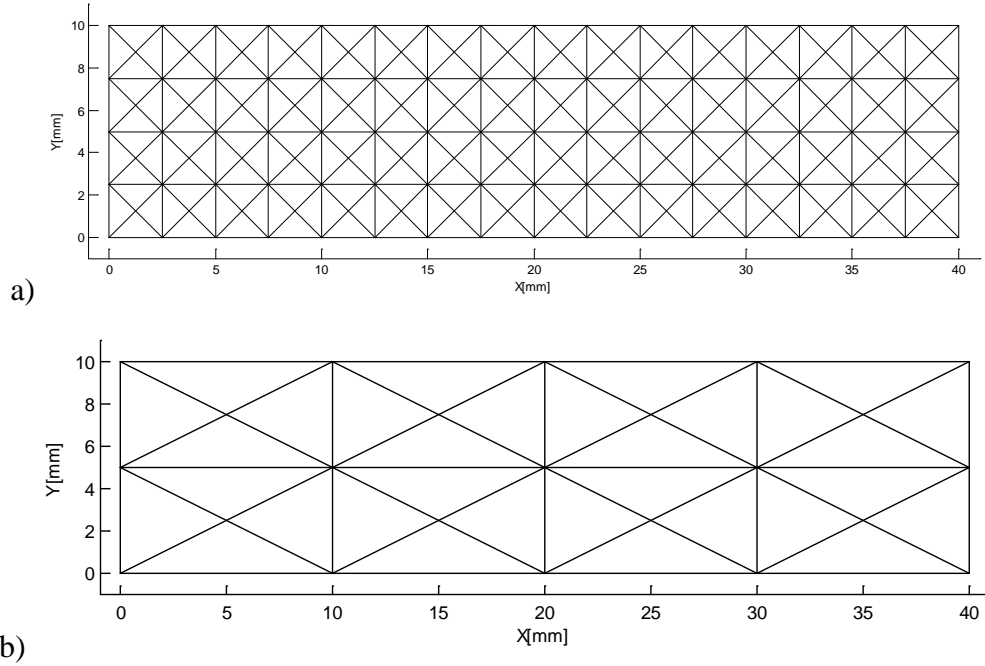
Figure 4-4: Different unit-cell sizes a) 2.5 × 2.5 mm b) 5 × 10 mm
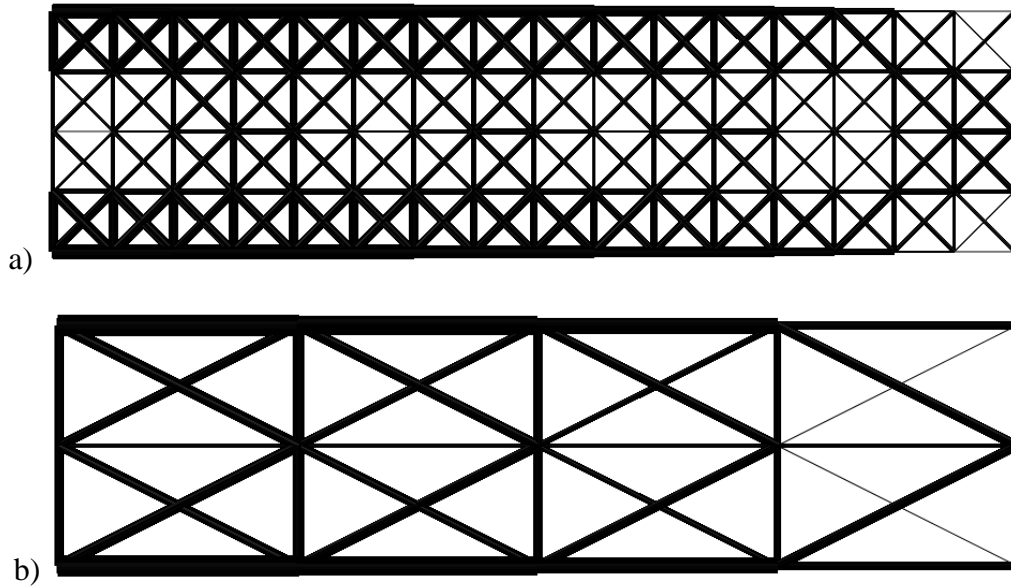
Figure 4-5: Generated optimized lattice structures a) 2.5 × 2.5 mm b) 5 × 10 mm

The 5 × 10 mm design had less displacement than the 5 × 5mm design, but the 2.5 × 2.5 mm had more. This can be related to two things; the size of the elements used in the topology optimization and how well does the crossed lattice structure conform to the topology optimization results. Figure 4-6 shows the generated lattice structures of the 3

size mapped on the topology optimization results. It is clear from the figure that the 5 ×10 mm design conformed well to the topology optimization results and had more elements contributing to the strut. The 2.5 × 2.5 mm design had the struts' diameters determined a small number of elements, which caused struts that are in a void region but close to a solid element to have a noticeable relative area. This observation indicates that the size of the unit-cells and configuration, along with the element size of the topology analysis, affects the performance of the structure.
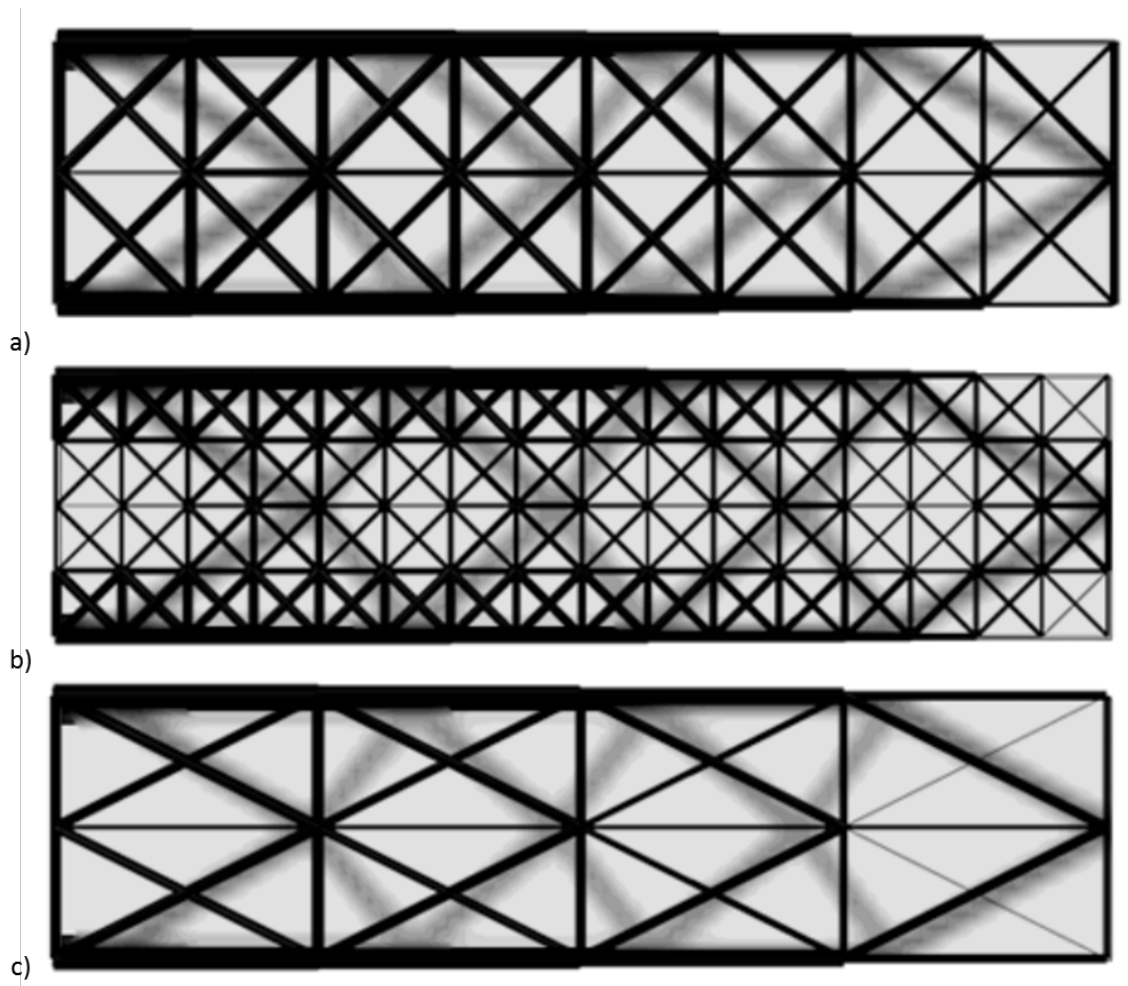
Figure 4-6: Lattice structure mapping on the topology optimization results a) 5 × 5mm

b) 2.5 × 2.5mm c) 5 × 10mm

Table 4-3: Tip displacement using RDM at different unit-cell sizes

Size (mm)	Tip displacement (mm)
5 × 5	0.48
2.5× 2.5	0.66
5 × 10	0.44

4.1.5   Effects of Ar_l and RR

To investigate the effects of Ar_l and RR on the performance of the design, the 5 × 5 mm design was analyzed under different values of Ar_l and RR. Ar_l had values change from 0.05 to 0.15, while RR from 0.001 to 0.2 to see their effect on the tip displacement of the generated lattice structure. Figure 4-7 shows the change in the tip displacement with these different values. The increase in RR causes a decrease in the tip displacement until the value becomes large enough to cause removal of essential struts. The values of Ar_l on the other hand, cause an increase in the tip displacement, so small values of Ar_l are preferred as well. It can be seen in the figure that the values 0.05 for Ar_l and 0.1 for RR have the lowest displacement when compared to the other values, even though the change is not that much; but for different sizes, there was a noticeable change as shown in figure 4-7 and 4-8.
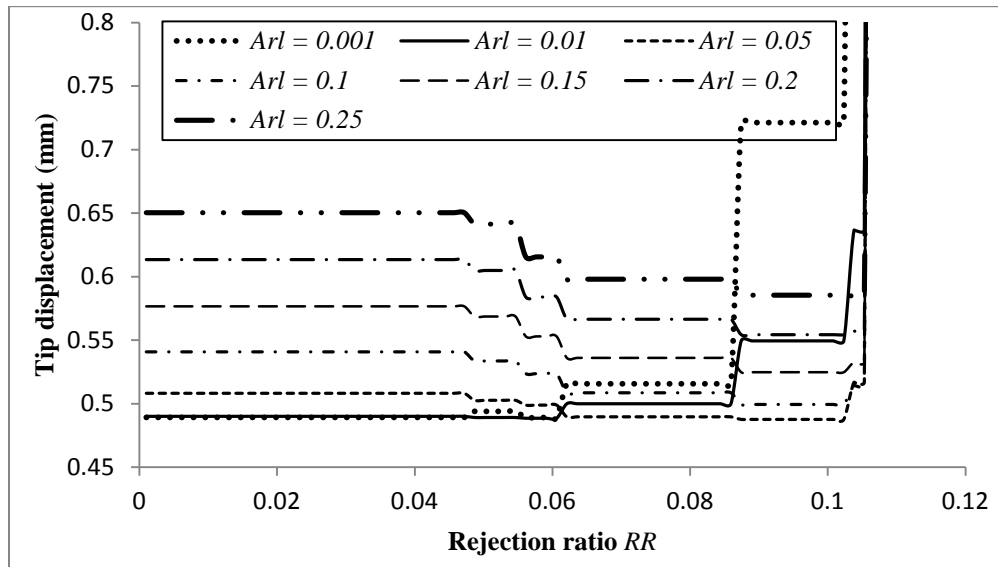
Figure 4-7: Effect of the values of RR on the tip displacement at different Ar_l values (5 × 5)
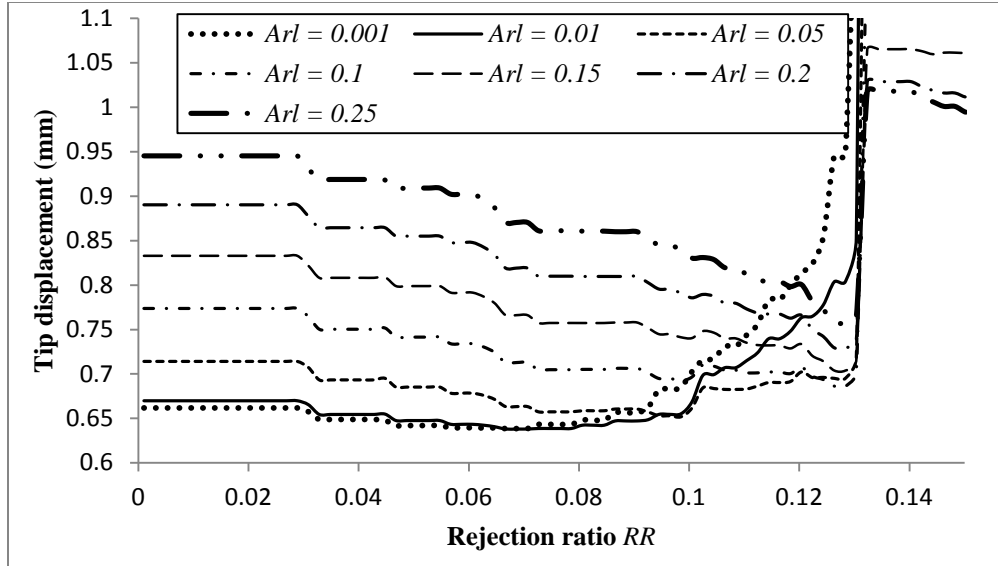
Figure 4-8: Effect of the values of *RR* on the tip displacement at different *Ar_l* values (2.5 × 2.5)
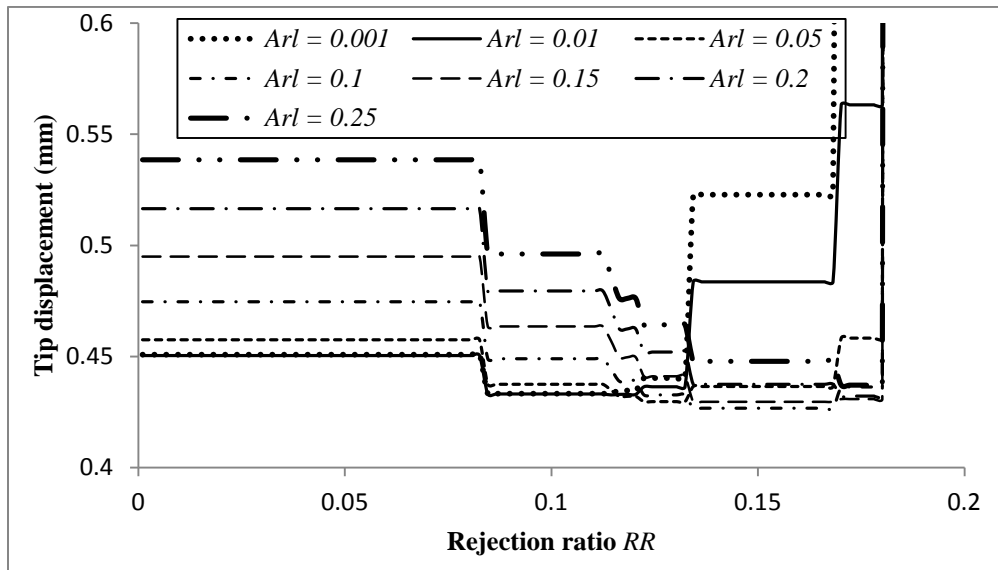
Figure 4-9: Effect of the values of *RR* on the tip displacement at different *Ar_l* values (5 × 10)

From Figure 4-9, the design had the lowest tip displacement with *Ar_l* value of 0.1 and *RR* value of almost 0.15. The tip displacement is larger than in the design in Figure 4-7. The figures also show that with small *Ar_l* values, increasing *RR* reduces the tip displacement, but after a certain value it causes an increase in the tip displacement to increase faster. Based on these observations, for the next examples, a value of *Ar_l* = 0.01 and *RR* = 0 will

50

be used. The omitting of the screening process, is due to its small decrease in the deformation for small Ar_l Values

4.1.6 Summary

The example showed how the RDM method is used in the design process of lattice structures. The optimized structure is affected by the choice of Ar_l, *RR,* and the size of the unit-cells and configuration. For further examples, a value of $Ar_l = 0.01$ and $RR = 0$ will be used.

4.2 3-D Curved Cantilever Beam

4.2.1 Problem Description

The Second example is a 3-D curved cantilever beam. The problem was investigated in the work done by Nguyen [53] to evaluate the performance of the SMS method in curved surfaces. The beam is fixed at one end and subjected to two concentrated loads at two points in the Z-direction on the other end. The beam is shown in Figure 4-10.
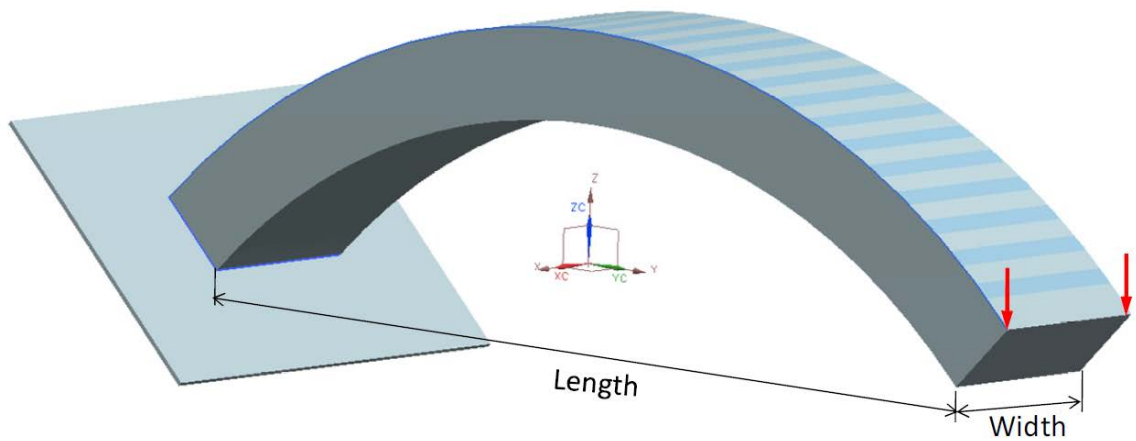
Figure 4-10: 3-D curved cantilever beam

The properties of the beam are shown in Table 4-4. The goal of the example is to evaluate the performance of the RDM method with SMS. The target volume of the desired structure is 5000 mm^3.

51

Table 4-4: Curved cantilever beam properties

Outer radius (mm)	84.5
Inner radius (mm)	74.5
Width (mm)	20
Length (mm)	105
Loading magnitude (N)	1
Modulus of Elasticity (MPa)	1960
Unit-cell size in-plane (mm)	10
Unit-cell size out-plane (mm)	10
Target volume (mm^3)	5000

4.2.2 Solid Model Topology Optimization

The topology optimization of the solid model was conducted in ABAQUS/ATOM. The mathematical formulation of the topology optimization is as follows:

$$\text{min} \qquad U(\boldsymbol{\rho}) = \frac{1}{2}\sum_{i=1}^{n}\mathbf{u}_i^T \mathbf{K}_i \mathbf{u}_i$$

$$\text{Subject to} \quad \sum_{i=1}^{n}\rho_i V_i \leq 5000 mm^3 \qquad (4\text{-}1)$$

$$0 \leq \rho \leq 1$$

Figure 4-11 shows the isosurface of the optimization process in ABAQUS/ATOM. Elements with values of $\rho \leq 0.3$ were removed to identify what elements of the solid model would contribute more in the creation of the lattice structure. Figure 4-12 shows the contour plot of the relative density of the material. The plot shows that elements on the sides of the upper portion will contribute more in increasing the structure's stiffness, while on the bottom side, the elements in the center are more critical.
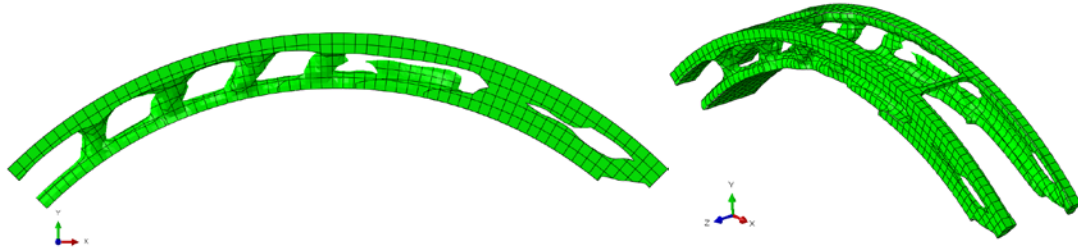
Figure 4-11: Isosurface of the optimized curved beam
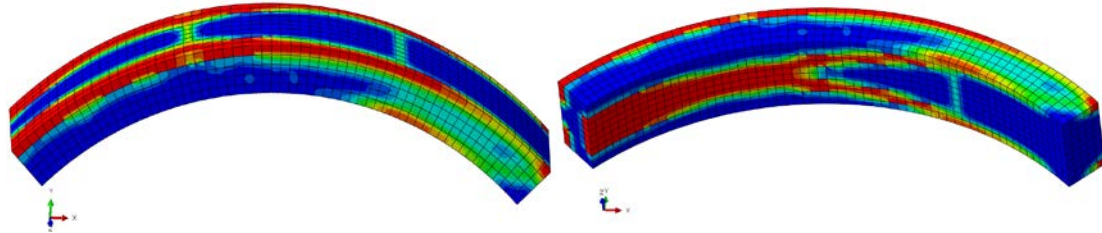
Figure 4-12: Relative density contour plot of the curved beam

4.2.3 Generating the Lattice structure

The base unit-cells of the lattice structure of the design problem are shown in Figure 4-13. By mapping the information obtained from the topology optimization of the solid model, the lattice structure is generated using RDM method as shown in Figure 4-14.
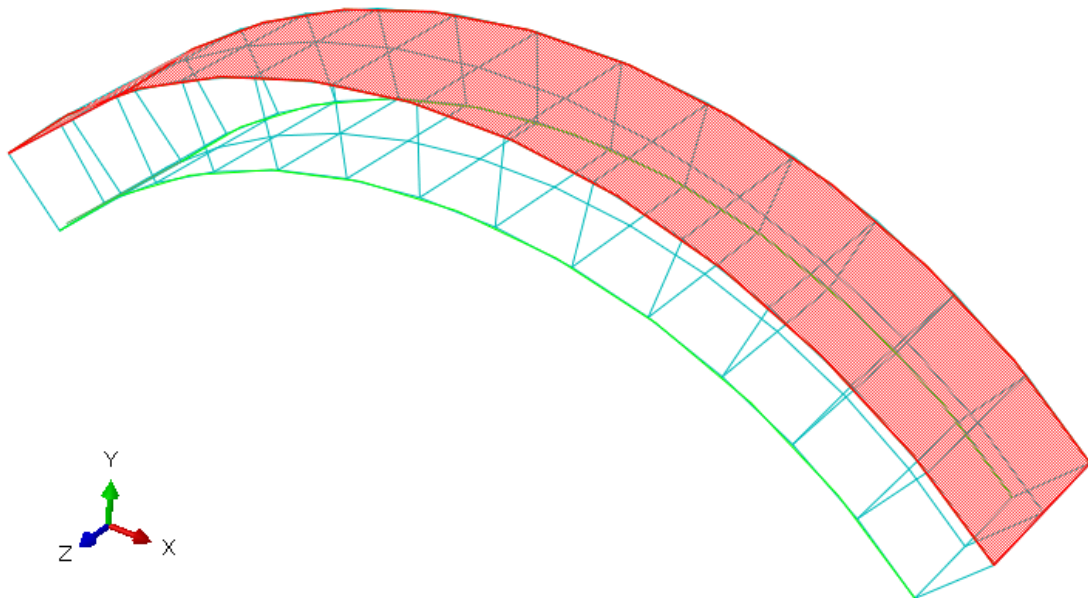
Figure 4-13: Base-lattice structure of the curved cantilever beam
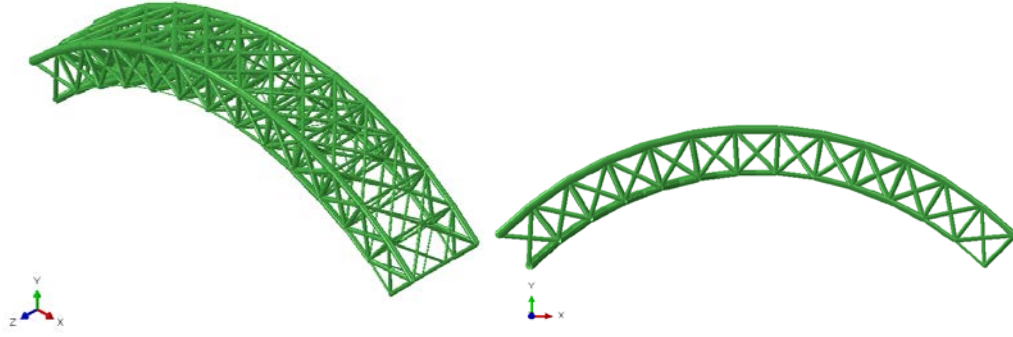
Figure 4-14: Generated lattice structure for the curved beam

4.2.4 Comparison of the Results

The results of the tip displacement of the RDM lattice structure and other methods are shown in Table 4-5. An equally sized lattice structure was analyzed and found to have a maximum tip displacement of 3.109 mm. This value serves as a top boundary on the maximum tip displacement for the lattice structure generated by the other methods. The Active-set optimization algorithm of the ground structure approach was utilized using equation 4-1 to evaluate the performance of the method. The ground structure model had a maximum tip displacement of 0.6014 mm and required 16,593 FEM simulations. The results of the SMS method were presented in the work done by Nguyen [53]. Active-set and LM algorithms were used in the SMS lattice structure along with a 28% assumption on the diameter ratio of the lattice structure. The 28% assumption had a maximum tip displacement of 2.2298 mm. The number of FEM simulations required for the SMS with active-set and LM were not available, but rather the time required for the simulation; so the results were not presented in Table 4-5. But it would require more FEM simulations. The tip displacement was the same for both methods. The RDM method produced a tip displacement of 2.144 mm, which is better than the 28% assumption in SMS, but if the topology optimization results were not present, it would require 47 FE simulations.

Table 4-5 Optimization results of the curved beam

Method	Tip displacement (mm)	No. of Simulations	
Identically sized structure	3.109	-	
Ground structure (Active-set)	0.6014	16593	
SMS (28% assumption)	2.2298	-	
SMS (Active-set)	1.9501	N/A	
SMS (LM)	1.9501	N/A	
RDM ($Ar_l = 0.01$)	2.147	-	47

4.2.5 Summary

The example was used to demonstrate the performance of the RDM method with SMS using the crossed unit-cell. The method performs well when compared to the SMS (28% assumption) method and shows a relatively comparable results. SMS with active-set and LM optimization algorithms performed slightly better but with the cost of the increase in the number of FEM simulations required.

4.3 Multi Load Case Cantilever Beam

4.3.1 Problem Description

This example will demonstrate the advantage of the RDM method over SMS method when dealing with more than one load case. The example is a rectangular beam with 50 mm length, 20 mm height, and 10 mm width. It is fixed at one end and subjected to a transverse load on the other end (Figure 4-15). The properties of the beam are shown in Table 4-6. The example was investigated in [53] in only one load case Figure 4-15-a. A second load case was added (Figure 4-15-b) to evaluate the performance of the generated lattice structures in in handling two loading cases.

Table 4-6 Cantilever beam properties

Length (mm)	50
Height (mm)	20
Width (mm)	10
Loading magnitude (N)	10
Modulus of Elasticity (MPa)	1960
Unit-cell size (mm×mm)	10×10
Target volume (mm^3)	1600
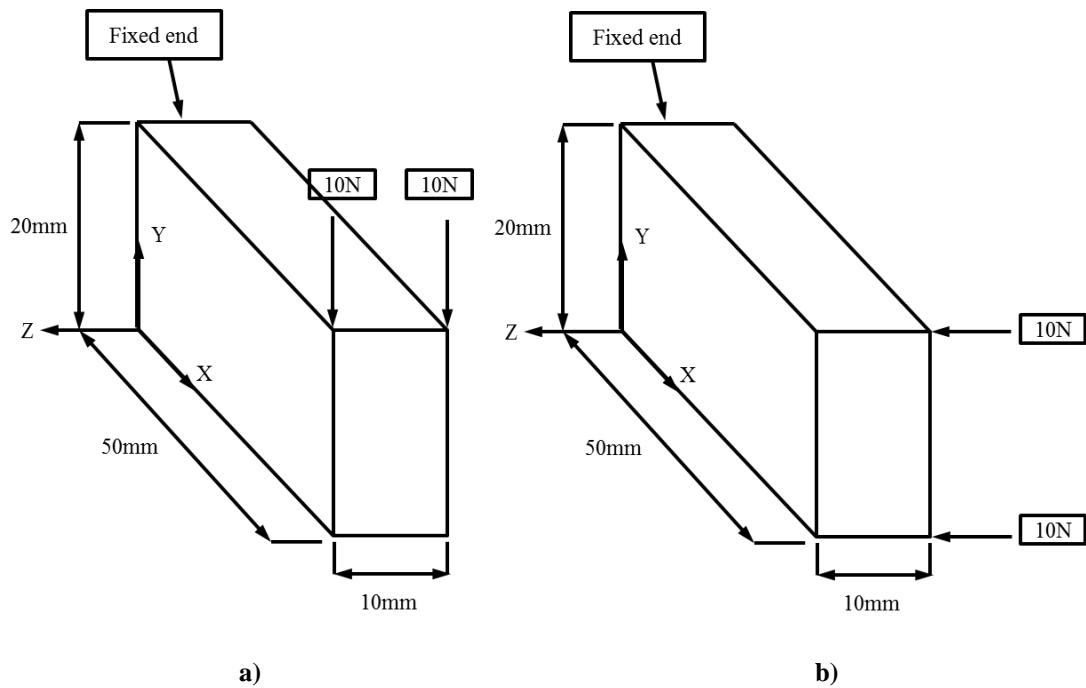
Figure 4-15 Cantilever beam a) Load case 1 b) Load case 2

4.3.2 Solid Model Topology Optimization

The solid model was created in ABAQUS to generate the optimized model and extract the relative density information. The optimization was carried using ABAQUS/ATOM as follows:

$$\min \qquad U_1(\mathbf{\rho}) + U_2(\mathbf{\rho})$$

$$\text{Subject to} \quad \sum_{i=1}^{n} \rho_i V_i \leq 1600mm^3 \qquad\qquad (4\text{-}2)$$

$$0 \leq \rho \leq 1$$

where U_1 and U_2 are the strain energies for load case 1 and 2 respectively. Figure 4-16 shows the isosurface of the optimized model (elements with $\rho < 0.3$ are removed). Figure 4-17 shows the contour plot of the relative density of the model.
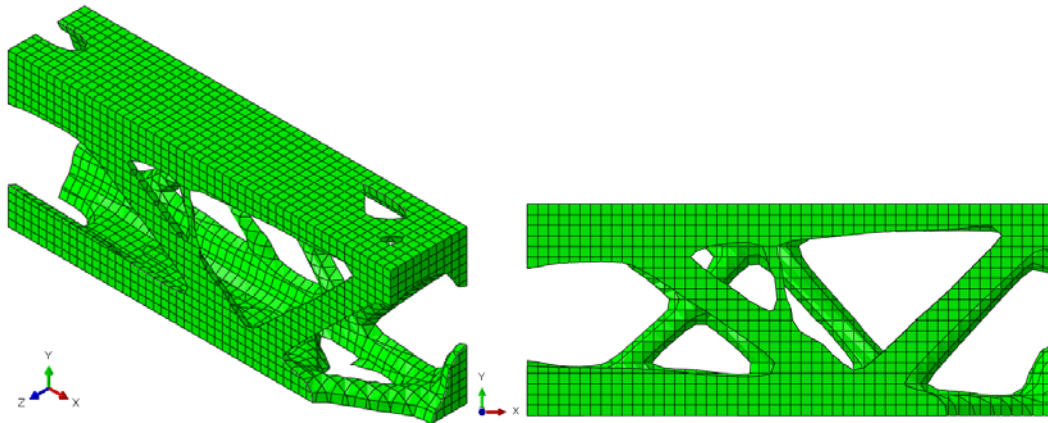
Figure 4-16 Isosurface of the optimized cantilever beam
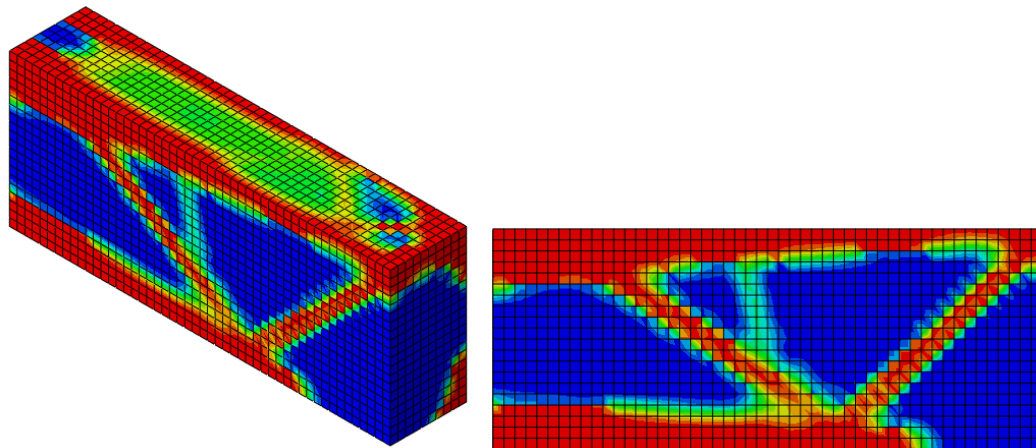
Figure 4-17 Relative density contour plot

4.3.3 Generating the Lattice Structure

The base unit-cells are generated as shown in Figure 4-18. The relative density information was then implemented in the MATLAB code to generate the lattice structure with *AR* value of 0.01 as shown in Figure 4-19.
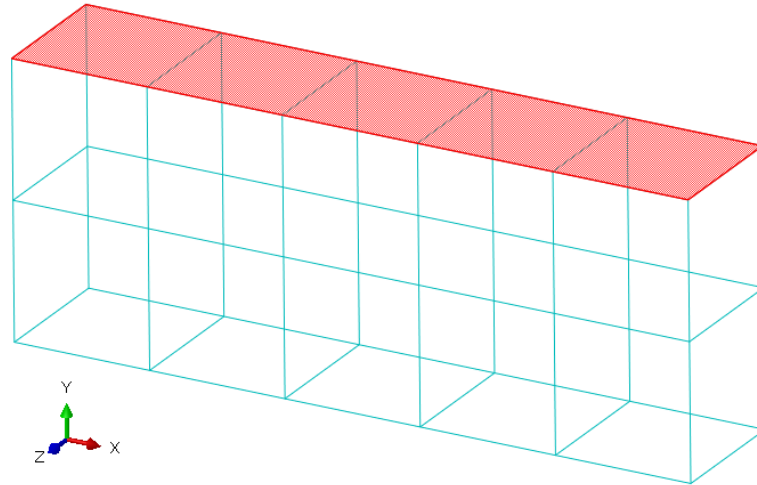
Figure 4-18 Base unit-cells of the cantilever beam
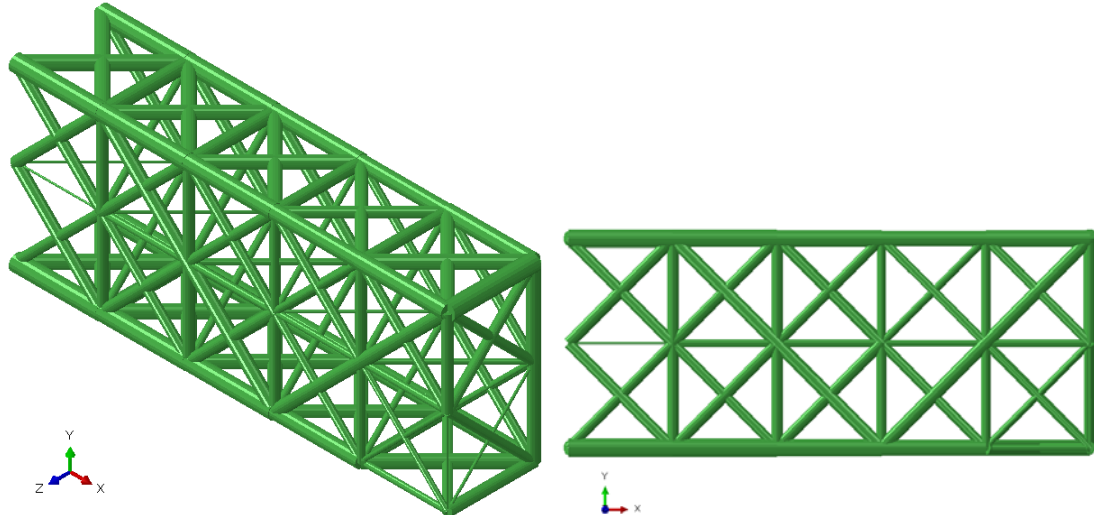
Figure 4-19 Generated lattice structure for the cantilever beam

4.3.4 Comparison of the Results

To evaluate the performance of the structure, the maximum tip displacement in both load cases was obtained with different methods. An identically sized structure was generated

to act as an upper bound to determine how well does the methods perform with respect to it. The ground structure model was optimized using active-set optimization algorithm to evaluate how well the methods perform compared to it, and how many FEM simulation cost will be saved by doing so. The augmented SMS method using active-set algorithm, since it only works with one load case, was used 3 times. The first lattice structure was generated using the FEM results of load case 1. The second is generated using load case 2 results. As for the third model, the combined load cases FEM results were used. The results of the optimization processes are shown in Table 4-7.

Table 4-7 Results of the optimization methods of the cantilever beam

<table>
<tr><td colspan="2">Method</td><td>Displacement Y (mm)</td><td>Displacement Z (mm)</td><td colspan="2">No. of Simulations</td></tr>
<tr><td colspan="2">Identically sized structure</td><td>1.21</td><td>2.837</td><td colspan="2">-</td></tr>
<tr><td colspan="2">Ground structure (Active-set)</td><td>0.5795</td><td>0.9762</td><td colspan="2">6418</td></tr>
<tr><td rowspan="3">Active-Set</td><td>SMS (Load case 1)</td><td>0.6234</td><td>29.1</td><td colspan="2">82</td></tr>
<tr><td>SMS (Load case 2)</td><td>3.668</td><td>6.2</td><td colspan="2">35</td></tr>
<tr><td>SMS (combined Loads)</td><td>3.024</td><td>7.626</td><td colspan="2">38</td></tr>
<tr><td rowspan="3">LM</td><td>SMS (Load case 1)</td><td>0.6225</td><td>29.3</td><td colspan="2">60</td></tr>
<tr><td>SMS (Load case 2)</td><td>3.668</td><td>6.2</td><td colspan="2">69</td></tr>
<tr><td>SMS (combined Loads)</td><td>3.024</td><td>7.626</td><td colspan="2">78</td></tr>
<tr><td colspan="2">RDM ($Ar_l = 0.01$)</td><td>0.678</td><td>1.827</td><td>-</td><td>80</td></tr>
</table>

4.3.5 Summary of Results

The results in Table 4-7 shows that the RDM method performs even better than the SMS method when considering multiple load cases. The displacement in the *Z* direction for the RDM method is almost 2 times that of the ground structure approach. But the reduction in the simulation cost and the relatively close performance in the *Y* direction show the potential of the method in saving time cost and obtaining a reliable design. The SMS method performed poorly in the *Z* direction when only considering the second load case which also affected the displacement in the *Y* direction. This was due to the large unit-cell

size compared to the solid model, which affected the process of mapping stresses to the unit-cells. Combining both loads reduced the displacement in the Y direction, but increased it in the Z direction, since the method will have to take into two accounts the two loads that are acting. But it is still large when compared to the identically sized structure.

4.4 Practical Example (Design of an Elevator Sling component)

4.4.1 Problem description

This example will demonstrate the application of RDM in optimizing the structure of an elevator cab sling component. Figure 4-20 shows a picture of different components of a sling that is used in an elevator. The component that will be optimized is the bolster which carries a load of 2250 kg that is distributed on its surface. A CAD model of the bolster is shown in Figure 4-21. The bolster is made of steel with and elastic modulus of 210 MPa and a density of 7700 kg/m^3 dimensions of the bolster are shown in Figure 4-22.
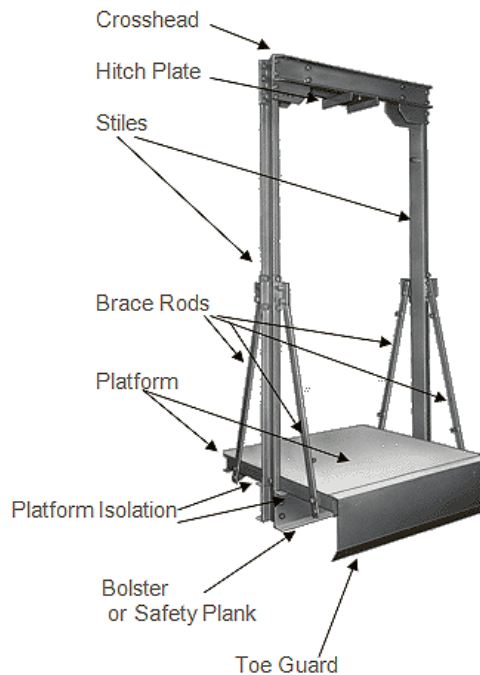
Figure 4-20 Elevator sling components [54]
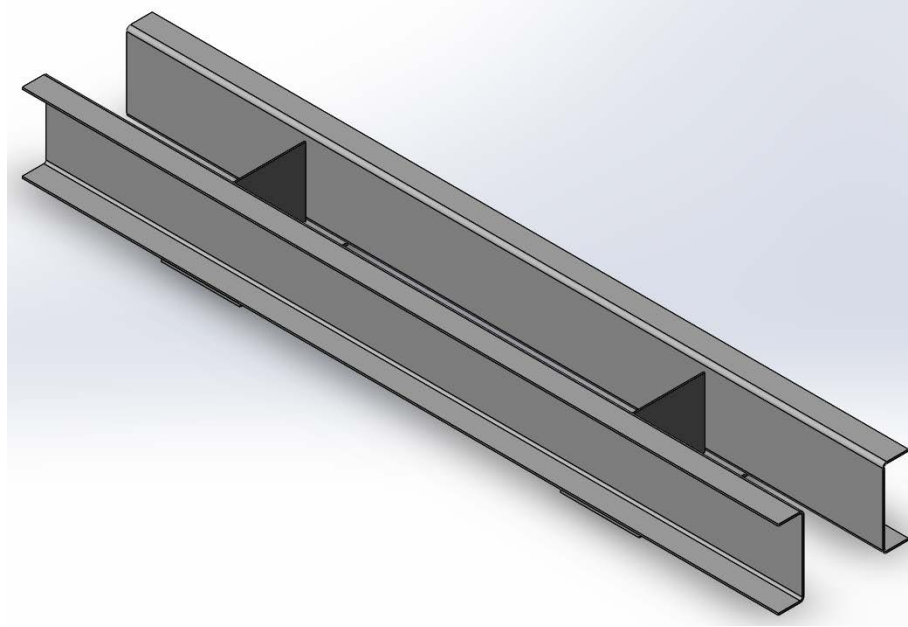
Figure 4-21 CAD model of the bolster
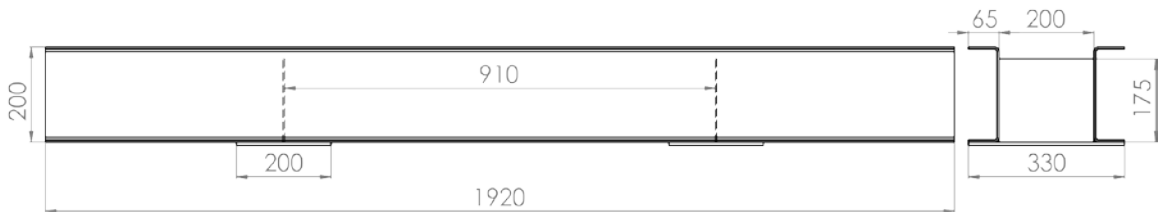
Figure 4-22: Dimensions of the bolster (mm)

The bolster (shown in Figure 4-21) is made of two 1920m long 200×65×4.5 mm C-channels back to back, two 200×175×3.5 mm plates in the transverse direction, two 330×8×6.5 in plates under the C-channels (Figure 4-22). The total weight of the bolster is 51.26 kg. The bolster was analyzed using FEM in ABAQUS. The sides are assumed to be fixed, and a pressure loading of magnitude of 0.1 MPa was applied on the top surface of the bolster to act as the distributed 2250 kg (Figure 4-23). Figure 4-24 shows the FEM model of the sling bolster. One fourth of the model was analyzed, due to the symmetry of the model and proper symmetry boundary conditions were applied where needed. 1060 quadratic shell element of type S8R were used in the C-channels and 180 elements were used on the supporting plates. The average element size for both components is 18×18 mm.
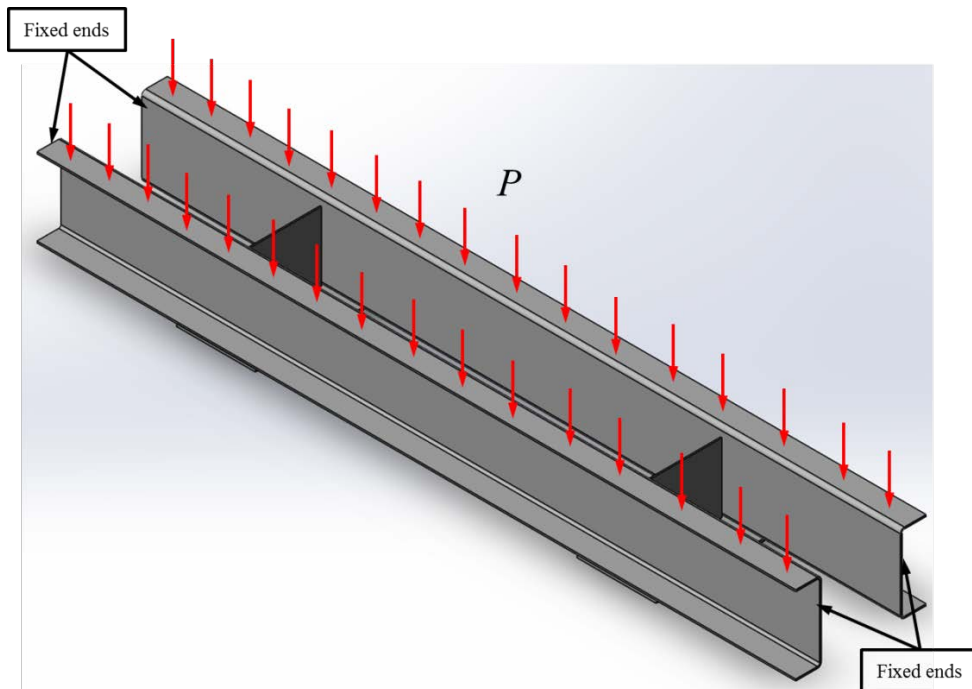
Figure 4-23 Loads and boundary conditions on the bolster
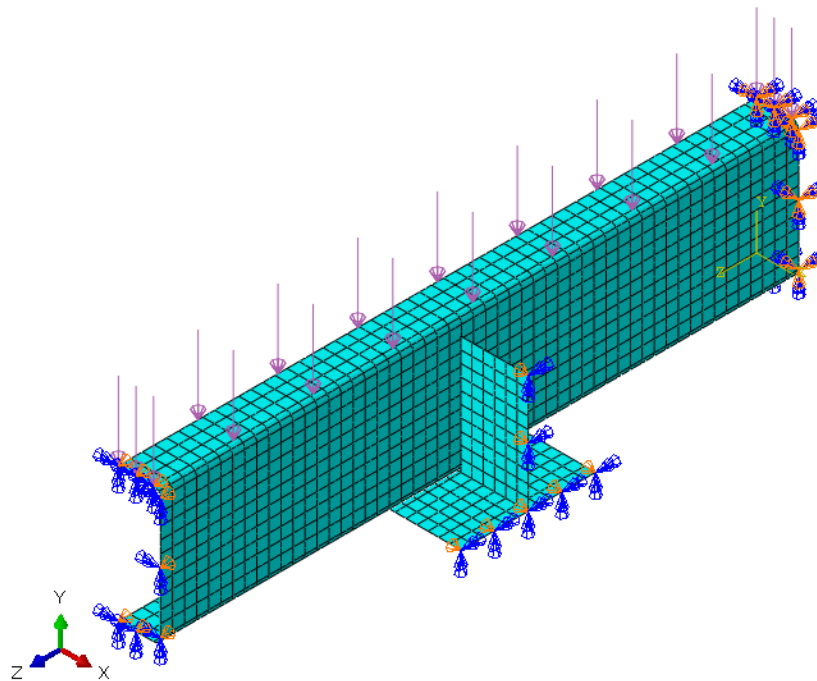
Figure 4-24 FEM model of the bolster

The FEM results show that the bolster had a maximum deflection on the C-channel of 1.02 mm on the C-channel (Figure 4-25).
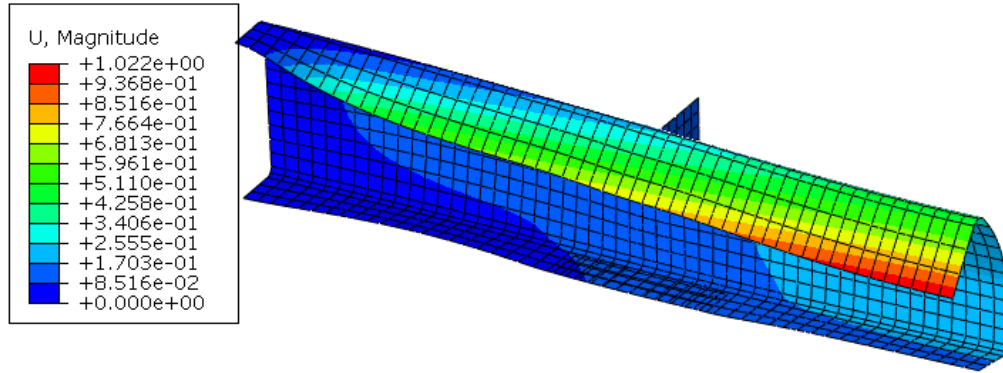
Figure 4-25 Maximum deflection on the bottom channel

4.4.2 Solid Model Topology Optimization

A solid fixed-fixed block of dimensions $330 \times 200 \times 1920$ mm was created to conduct the topology optimization as shown in Figure 4-26. The model was subjected to a pressure loading of 0.036 MPa, which corresponds to the distributed 2250 kg loading. The model was optimized as follows:

$$\min \qquad U(\boldsymbol{\rho}) = \frac{1}{2} \sum_{i=1}^{n} \mathbf{u}_i^T \mathbf{K}_i \mathbf{u}_i$$

$$\text{Subject to} \quad \sum_{i=1}^{n} \rho_i V_i \leq 0.2V' \, mm^3 \qquad (4\text{-}3)$$

$$0 \leq \rho \leq 1$$
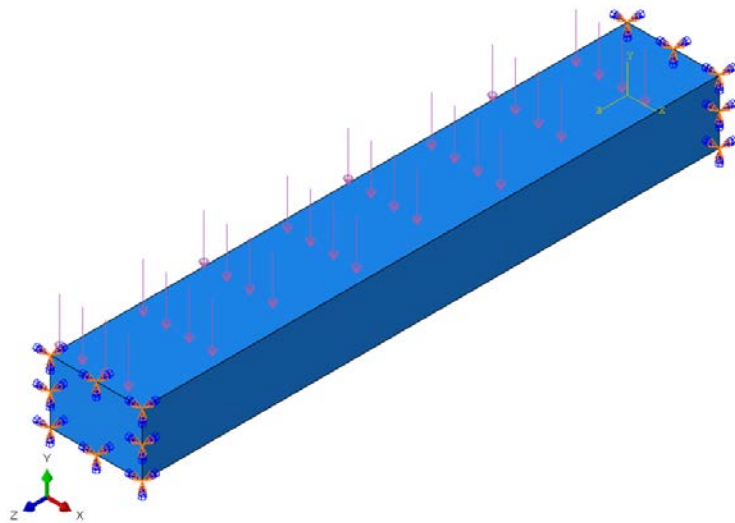
Figure 4-26 Sling bolster solid model

63

Figure 4-27 shows the isosurface extracted from the topology optimization. Figure 4-28 shows the contour plot of the relative density.
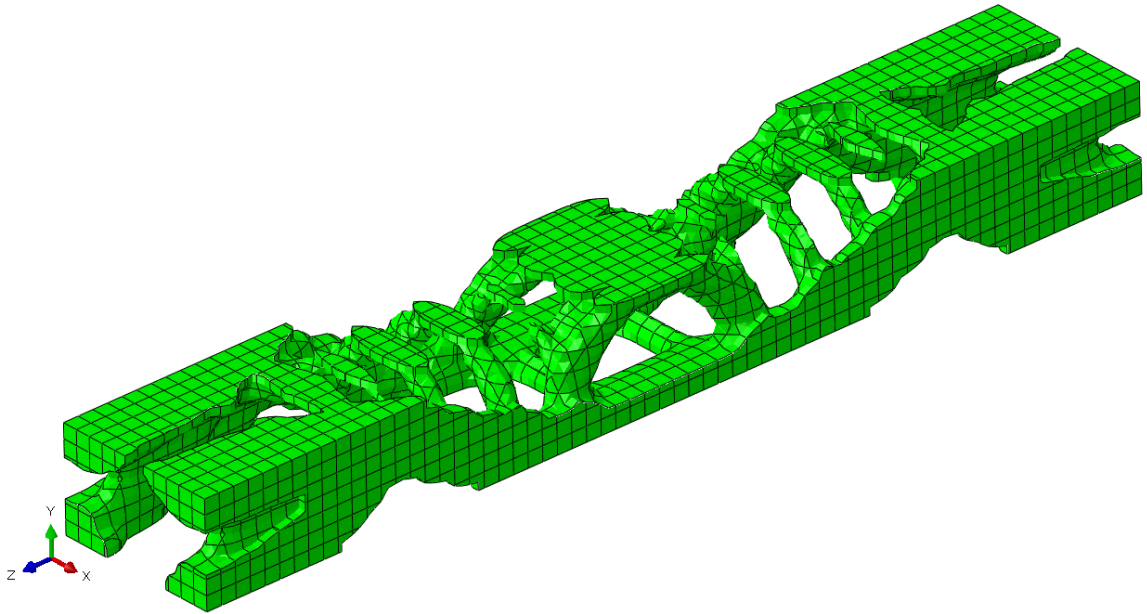
Figure 4-27 Isosurface of the optimized solid model
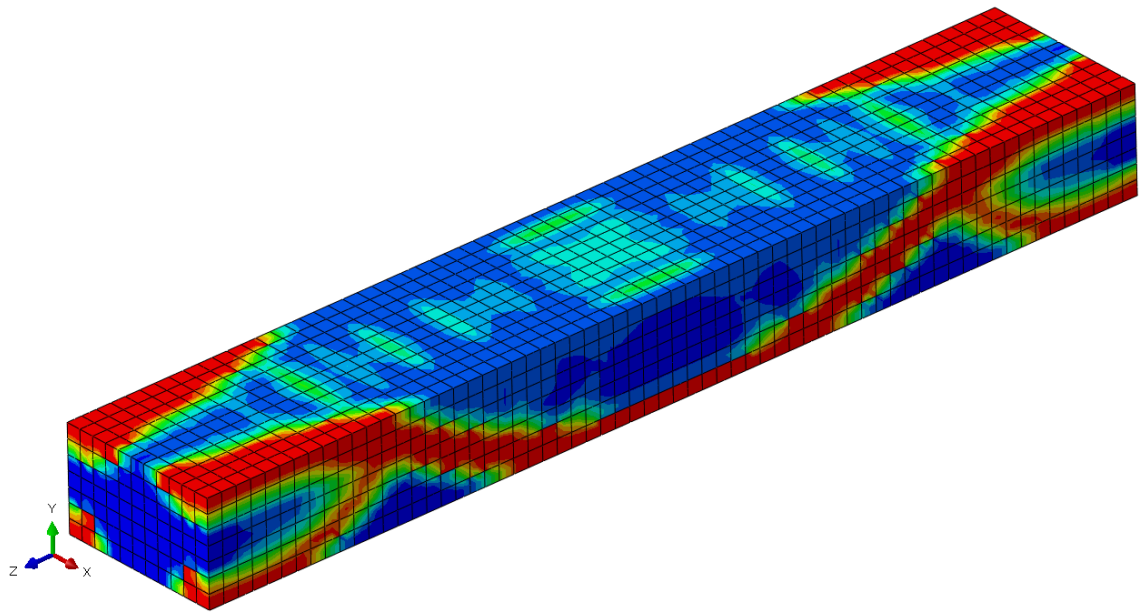
Figure 4-28 Relative density contour plot

4.4.3 Generating the lattice structure

Nine base unit-cells were generated for the design as shown in Figure 4-29. Using the density information obtained from the topology analysis, the lattice structure was created with Ar_l value of 0.01 (Figure 4-30). The structure was generated while maintaining the weight constraint of 51.26 kg.
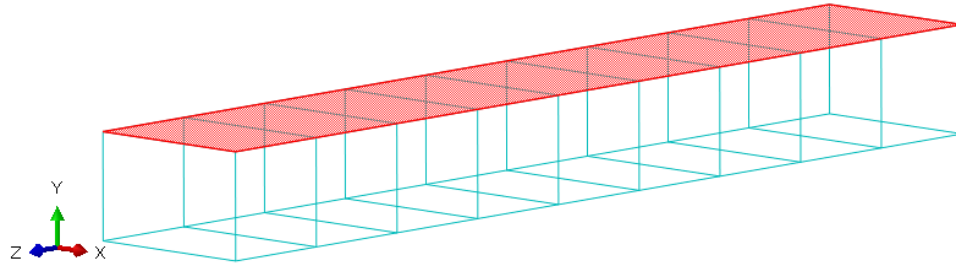
Figure 4-29 Base unit-cells of the sling bolster
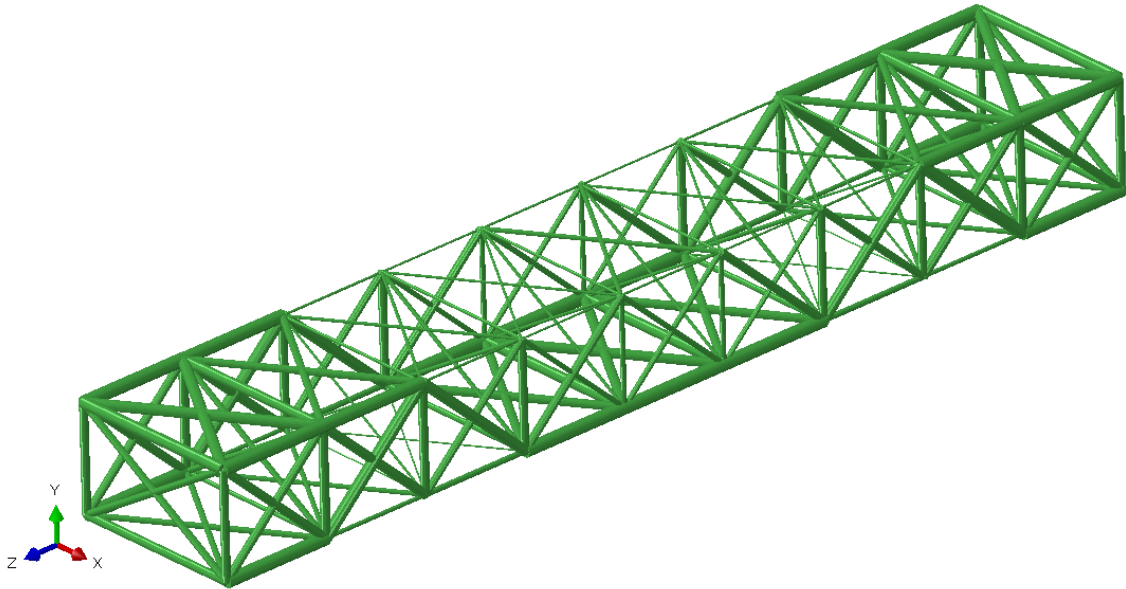
Figure 4-30 Generated lattice structure of the sling bolster

4.4.4 Analysis Results

To evaluate the performance of the generated lattice structure, an identically sized structure was generated to act as an upper bound, and a ground structure model was

optimized with active-set algorithm to see how far is the structure generated by RDM is from the ground structure model. The results of the analysis are shown in Table 4-8.

Table 4-8 Analaysis results of the sling bolster

Method	Tip displacement (mm)	No. of Simulations	
Current steel structure	1.02	-	
Identically sized structure	0.5128	-	
Ground structure (Active-set)	0.1945	16936	
RDM ($Ar_l = 0.01$)	0.325	-	49

4.4.5 Summary of the Results

The results show that the RDM method provided a better solution to the pre-existing design for the sling bolster and would require 49 FE simulations for the topology optimization process. The ground structure approach using active-set algorithm had higher stiffness, but required an extensive amount of FEM simulations to reach this value.

4.5 Summary

This chapter provided 4 examples to evaluate the performance of RDM with different cases. The first example was used to investigate the effects of the different parameters in the method on the performance of the generated structure. The size of the unit-cells showed an effect on the tip deflection of the generated lattice structure. Also, how well the struts conform to the topology results show an improvement in the response. The values of the parameters Ar_l and RR also had an effect on the lattice structure's performance. RR increases the stiffness of the structure, but at large values it can remove struts with small diameters in critical areas that will cause sudden increase in the deflection of the tip. The values of Ar_l on the other hand, reduce the stiffness of the structure but can help prevent the sudden increase in deflection at RR values. It can slow the occurrence of this behavior in the structure. Determination of the optimal values of these parameters can be an area for future investigation.

The second example was used to compare the performance of RDM with SMS and the ground structure approach. The results produced by RDM were better than SMS with the assumption of 28% on the diameters ratio. But the other values of SMS that used an optimization process to determine the minimum and maximum diameters had slightly better results, but at the expense of the number of simulations required.

The third example was used to evaluate the performance of RDM, SMS, and ground structure approach on the design of structures that are subjected to two loading conditions. RDM showed great results when compared to SMS. SMS with the consideration of the first loading condition had a weak resistance to the second load applied to it. When the second loading condition was considered alone, SMS produced poor results, since only one element was used across the width of the beam and five across the beam span. This caused a huge variation in the stress values inside one unit-cell. Combining the two load cases, still suffered from this problem in SMS. The ground structure produced the lowest displacement but with a large number of FEM simulations.

The last example was a demonstration of applying RDM in the design of an elevator bolster. The current design was analyzed using FEM to compare the results with the design generated using RDM. Both designs were constrained to the same mass. RDM generated a design that was stiffer than the current design.

CHAPTER 5

CONCLUSIONS AND FUTURE WORK

5.1 Summary

Due to the advances in additive manufacturing, design complexity is no longer an issue to consider in relation to manufacturing. Parts of complex geometry and even material composition can be produced with AM technology. Types of structures known as cellular structures, specifically lattice structures, are used for the design of light-weight and stiff components. These structures are manufactured to contain material where it is needed for its application purpose. Several design approaches have been investigated and pointed out in this research. One of these approaches is the SMS method that utilizes solid-body FEA. The major drawback of this method, as pointed out in the research, is that it's limited to the loading condition it was designed for.

A new method for the design of lattice structures was proposed in this research that will utilize the relative density information obtained from topology optimization for designing lattice structures. The utilization of this information will not limit the design method to only one loading condition. The method performs by mapping the relative density information to a strut in the predefined lattice structure from neighboring FE elements. This allows the determination of the relative cross-sectional area of each strut in the structure. The unit-cell that was utilized in the analysis is the crossed type. After the determination of the relative cross-sections, the lattice structure is then scaled to meet the volumetric design requirement.

Chapter 2 of the research is a literature survey on the design approaches for cellular structures and a detailed part on topology optimization. Also the small section on optimization algorithms that were utilized in the research was presented.

Chapter 3 shows the process of how the RDM method was formulated and a detailed overview of the design steps using the RDM method. An algorithm was created to help implement the generation of lattice structures using MATLAB.

Chapter 4 shows examples of the application of the RDM method in 2-D and 3-D problems. Another example was used to demonstrate the performance of the generated lattice structure in a multi loading condition problem. The last example was a practical example on using the method to design an elevator sling bolster.

Chapter 5, which is this chapter, provides a summary of the work done, conclusions and future work that will be done.

5.2 Conclusions

The RDM method presented in this work shows great potential for designing lattice structures. The first example showed the effects of different unit-cell sizes on the performance of the structure. It showed better performance when the lattice structure had struts that are conformal to the topology optimization results. Smaller sized unit-cells performed weaker due to the fact that a small number of topology optimization elements were effectively mapped to the struts. It also showed the effect of the parameters Ar_l and RR on the performance of the structure. The increase in Ar_l tends to reduce the stiffness of the part, but it increases its resistance to sudden decrease in stiffness when the values of RR increase.

Results of the second example shows that RDM performs well when compared with the results obtained from SMS with 28% assumption. SMS have slightly better results than RDM when using an optimization algorithm but at the expense of increased number of FEM simulations. Results from Nguyen's work [53] shows that different types of unit-cells for this example provided better results. This is a point for future investigation for the RDM method.

The third example shows the major advantage of RDM over SMS, which is generating lattice structures that are capable of handling different loading conditions. SMS however showed another drawback in this example. The structure that was generated to handle the second loading condition was pretty weak. This is due to the large size of the unit-cell when compared to the overall design region. This caused a problem in the correlation of solid-body FEM results to the unit-cells, since one unit-cell now is subjected to a huge variation in the stress values, unlike the case in the first example. In the first example, 14 unit-cells were over the span of the beam; while in the second example, only five. This wasn't a problem for the beam in the first load case, since it had two unit-cells across the beam's height. RDM method on the other hand, produced relatively comparable results with SMS for the first load case.

Overall the RDM can help in producing lattice structures with great performance and with no additional FEM simulations for the required part. But the determination of appropriate values for Ar_l and RR would require an optimization process to determine the best values for them. Another key point to be considered is that the size of the unit-cells should be relatively larger than the size of the FE elements used in the topology optimization. This will help in increasing the number of elements that will influence the cross-section of a strut.

5.3 Contributions

The method that was developed in this thesis allows the design of lattice structures. The major contribution of the method is that can be used for multiple loading conditions. This was a drawback for the SMS method, since the solid-body FEA is only limited to one loading condition. The developed method does not require additional FE simulations once topology optimization results are available nor does it require the topology analysis to be redone in order to be implemented in the method. This will allow the method to be integrated in commercial topology optimization software to design lattice structures.

5.4 Future Work

Some of the limitations that were found from the work done and the examples presented will be addressed in this section for future work in improving the method. Other points will also be addressed that can help in improving the method.

5.4.1 Different Weight Function Formulation

The weight function used in equation 3-2 only utilizes the distance r as a variable to determining the weight of each element in determining the strut's cross-section. Inclusion of other parameters such as, element's size, and direction cosines of r is an area of future investigation. Other areas include a using a different function than the exponential function to change how elements influence the struts.

5.4.2 Inclusion of Different Unit-cell Configurations

Only one type of unit-cell configuration was used in this research. Different types of configurations should be investigated and compared to the optimization results of SMS. A method for determining the optimal configuration for each unit-cell should also be investigated. A starting point would be finding which configuration conforms more to the topology optimization results. And also since cross-section of the struts is not dependent on the unit-cell configuration, different combinations of configurations won't cause complications in determining the cross-section values.

5.4.3 Determination of the Optimal Unit-cell Size

As shown in the first example, the results are affected by the size of the unit-cells and how well they conform to the topology optimization results. The base unit-cell size should be large enough to include more elements' relative density information to influence a single strut's cross-sectional area in the design.

5.4.4 Optimal Ar_l and RR values

The determination of the optimal Ar_l and RR value can be used in order to incorporate stress constraints on the design, since the increase of Ar_l will reduce stresses in the small cross-sectional area struts. But as pointed before, it can reduce the stiffness of the structure. Investigating a method for the determination of the best value for these parameters without requiring extra FEM simulations can enhance the performance of the method.

5.4.5 CAD Systems Integration

Since the method requires no constraints on the topology optimization process that is used, it can be integrated in commercial CAD systems to produce lattice structures after the topology optimization process has been conducted. This will give users the ability to design complex lattice structures at ease and no extra computational cost.

5.5 Closure

The long term goal of this research is to provide designers with a tool that is integrated in CAD systems and can help in designing lattice structures and to create structures that can be utilized in multiple loading conditions at no extra cost in the design time. This will help in involving lattice structures in industrial design; and with the advances in additive manufacturing, the geometric complexity is no longer a restriction on the fabrication of these structures.

REFERENCES

[1]   M. R. Legault and M. Musselman, "The rise of rapid manufacturing," *High Performance Composites*, vol. 17(4), pp. 32-37, July 2009.

[2]   D. W. Rosen, "Computer-aided design for additive manufacturing of cellular structures," *Computer-Aided Design & Applications*, vol. 4(5), pp. 585-594, 2007.

[3]   D. W. Rosen, I. Gibson and B. Stucker, *Additive Manufacturing Technologies: Rapid Prototyping to Direct Digital Manufacturing*. Springer, 2009.

[4]   A. Gebhardt, *Rapid Prototyping*. Munich: Hanser Publishers, 2003.

[5]   L. J. Gibson and M. F. Ashby, *Cellular Solids: Structure and properties*. Cambridge: Cambridge University Press, 1997.

[6]   M. F. Ashby and R. F. Mehl Medalist, "The mechanical properties of cellular solids," *Metallurgical Transactions A*, vol. 14(9), pp. 1755-1769, 1983.

[7]   M. F. Ashby, A. G. Evans, N. A. Fleck, L. J. Gibson, J. W. Hutchinson and H. N. G. Wadley, *Metals Foams: A Design Guide*. Burlington, MA: Butterworth-Heinemann, 2000.

[8]   V. S. Deshpande, N. A. Fleck and M. F. Ashby, "Effective properties of the octet-truss lattice material," *Journal of the Mechanics and Physics of Solids*, vol. 49(2001), pp. 1747-1769, 2001.

[9]   M. P. Bendsøe and O. Sigmund, *Topology Optimization: Theory, Methods and Applications*. Berlin: Springer, 2003.

[10]   J. P. Levia, "Topometry optimization: A new capability to perform element by element sizing optimization of structures," in *10th AIAA/ISSMO Multidisciplinary Analysis and Optimization Conference*, Albany, New York, 2004, pp.

[11]   "Image: TOSCA structure topology optimisation workflow," ed online: http://wildeanalysis.co.uk/fea/software/tosca

[12]   J. C. Medina and A. Tovar, "Topography optimization of shell structures under transient loading; a comparative approach," in *ASME IDETC/CIE 2012*, Chicago, Illinois, 2012, pp.

[13]   "Image: MSC Nastran topography optimization," ed online: http://www.mscsoftware.com/product/msc-nastran

[14]   "Image: Topometry optimization of a simple supported plate," ed online: http://www.genesis-support.com/examples/topometry-optimization-of-a-simple-supported-plate

[15]   G. C. Graf, J. Chu, S. Engelbrecht and D. W. Rosen, "Synthesis methods for lightweight lattice structures," in *ASME IDETC/CIE 2009*, San Diego, California, 2009, pp.

[16]   P. Chang and D. W. Rosen, "An improved size, matching and scaling method for the design of deterministic mesoscale truss structures," in *ASME IDETC/CIE 2011*, Washington, DC, 2011, pp.

[17]   J. Nguyen, S. Park and D. W. Rosen, "Heuristic optimization method for cellular structure design of light weight components," *International Journal of Precision Engineering and Manufacturing*, vol. 14(6), pp. 1-8, 2013.

[18]   J. C. Wallach and L. J. Gibson, "Mechanical behavior of a three-dimensional truss material," *International Journal of Solids and Structures*, vol. 38(pp. 7181-7196, 2000.

[19]   S. Chiras, D. R. Mumm, A. G. Evans, N. Wicks, J. W. Hutchinson, K. Dharmasena, H. N. G. Wadley and S. Fichter, "The structural performance of near-optimized truss core panels," *International Journal of Solids and Structures*, vol. 39(pp. 4093-4115, 2002.

[20]   S. R. Johnston, M. Reed, H. V. Wang and D. W. Rosen, "Analysis of mesostrucure unit cells comprised of octet-truss structures," in *Proceedings of the Seventeenth Solid Freeform Fabrication Symposium*, Austin, Texas, 2006, pp.

[21]   H. V. Wang, "A Unit Cell Approach for Lightweight Structure and Compliant Mechanism," PhD thesis, Georgia Institute of Technology, 2005.

[22] H. V. Wang, Y. Chen and D. W. Rosen, "A hybrid geometric modeling method for large scale conformal cellular structures," in *ASME Computers and Information in Engineering Conference*, Long Beach, California, 2005, pp.

[23] H. V. Wang, C. Williams and D. W. Rosen, "Design Synthesis of Mesoscopic Cellular Structures With Unit Truss Approach and Particle Swarm Optimization Algorithm," in *Proceedings of the The Seventeenth Solid Freeform Fabrication Symposium*, Austin, Texas, 2006, pp.

[24] A. G. M. Michell, "The limits of economy of material in frame structures," *Philosophical Magazine*, vol. 6(47), pp. 589-597, 1904.

[25] P. Dewhurst and S. Srithongchai, "An Investigaton of Minimum-Weight Dual-Material Symmetrically Loaded Wheels and Torsion Arms," *Journal of Applied Mechanics*, vol. 72(2), pp. 196-202, 2005.

[26] G. I. N. Rozvany, O. M. Querin, J. Lógó and V. Pomezanski, "Exact analytical theory of topology optimization with some pre-existing memebr or elements," *Structural Multidisciplinary Optimization*, vol. 31(5), pp. 373-377, 2006.

[27] S. V. Selyugin, "On optimal geometrically non-linear trusses," *Structural Multidisciplinary Optimization*, vol. 29(2), pp. 113-124, 2005.

[28] W. Dorn, R. Gomory and H. Greenberg, "Automatic design of optimal structures," *Journal Mechanica*, vol. 3(pp. 25-52, 1964.

[29] D. Wang, W. H. Zhang and J. S. Jiang, "Combined shape and sizing optimization of truss structures," *Computational Mechanics*, vol. 29(4-5), pp. 307-312, 2002.

[30] S. A. Burns, *Recent advances in optimal structural design*, American Society of Civil Engineers, 2002.

[31] W. Achtziger, "On simultaneous optimization of truss geometry and topology," *Structural Multidisciplinary Optimization*, vol. 33(4-5), pp. 285-304, 2007.

[32] D. Wang, W. H. Zhang and J. S. Jiang, "Truss shape optimization with multiple displacement constraints," *Computer Methods in Applied Mechanics and Engineering*, vol. 191(33), pp. 3597-3612, 2002.

[33] T. Hagishita and M. Ohsaki, "Topology optimization of trusses by growing ground structure method," *Structural Multidisciplinary Optimization*, vol. 37(4), pp. 377-393, 2009.

[34] O. Sigmund, "A 99 line topology optimization code written in Matlab," *Structural Multidisciplinary Optimization*, vol. 21(2), pp. 120-127, 2001.

[35] A. R. Díaz and M. P. Bendsøe, "Shape optimization of structures for multiple loading conditions using a homogenization method," *Structural Optimization*, vol. 4(pp. 17-22, 1992.

[36] S. Johnsen, "Structural topology optimization," Master's thesis, Norwegian University of Science and Technology, 2013.

[37] O. Sigmund and J. Peterson, "Numerical instabilities in topology optimization: A survey on procedures dealing with checkerboards, mesh-dependencies and local minima," *Structural Optimization*, vol. 16(1), pp. 68-75, 1998.

[38] M. Rouhi, "Topology optimization of continuum structures using element exchange method," Master's thesis, Mississippi State University, 2009.

[39] G. I. N. Rozvany, "A critical review of established methods of structural topology optimization," *Structural Multidisciplinary Optimization*, vol. 37(3), pp. 217-237, 2009.

[40] M. P. Bendsøe, "Optimal shape design as a material distribution problem," *Structural Optimization*, vol. 1(4), pp. 193-202, 1989.

[41] G. I. N. Rozvany, M. Zhou and T. Birker, "Generalized shape optimization without homogenization," *Structural Optimization*, vol. 4(3-4), pp. 250-252, 1992.

[42] H. A. Eschenauer and N. Olhoff, "Topology optimization of continuum structures: A review," *Applied Mechanics Reviews*, vol. 54(4), pp. 331-390, 2001.

[43] K. Svanberg, "The method of moving asymptotes - a new method for structural optimization," *International Journal for Numerical Methods in Engineering*, vol. 24(pp. 359-373, 1987.

[44] S. Wang, "Krylov subspace methods for topology optimization on adaptive meshes," thesis, University of Illinois at Urbana-Champaign, 2007.

[45] K. Svanberg and M. Stople, "An alternative interpolation scheme for minimum compliance topology optimization," *Structural Multidisciplinary Optimization*, vol. 22(2), pp. 116-124, 2001.

[46] O. Sigmund and P. M. Clausen, "Topology optimization using a mixed formulation: An alternative way to solve pressure load problems," *Computer Methods in Applied Mechanics and Engineering*, vol. 196(13-16), pp. 1874-1889, 2007.

[47] M. P. Bendsøe and N. Kikuchi, "Generating optimal topologies in structural design using a homogenization method," *Computer Methods in Applied Mechanics and Engineering*, vol. 71(pp. 197-224, 1988.

[48] N. Gould, D. Orban and P. Toint, "Numerical methods for large-scale nonlinear optimization," *Acta Numerica*, vol. 14(pp. 299-361, 2005.

[49] "Matlab r2014a documentation, optimization toolbox: fmincon," ed. online: http://www.mathworks.com/help/optim/ug/fmincon.html

[50] W. H. Press, S. A. Teukolsky, W. T. Vettering and B. P. Flannery, *Numerical Recipes in C*. Cambridge, UK: Cambridge University Press, 1992.

[51] "Matlab r2014a documentation, optimization toolbox: lsqnonlin," ed. online: http://www.mathworks.com/help/optim/ug/lsqnonlin.html

[52] G. C. Graf, "Development of specialized base primitives for meso-scale conforming truss structures," Master's thesis, Georgia Institute of Technology, 2009.

[53] J. Nguyen, "A heuristic optimization method for the design of meso-scale truss structure for complex-shaped parts," Master's thesis, Georgia Institute of Technology, 2012.

[54] "Image: Car sling platform," ed online: http://www.stanleyelevator.com/hydraulic-elevator-modernization/